Frontiers of Information Technology & Electronic Engineering
www.jzus.zju.edu.cn; engineering.cae.cn; www.springerlink.com
ISSN 2095-9184 (print); ISSN 2095-9230 (online)
E-mail: jzus@zju.edu.cn

Event-triggered dynamic output-feedback control for a class of Lipschitz nonlinear systems*

Zhiqian LIU, Xuyang LOU†‡, Jiajia JIA

Key Laboratory of Advanced Process Control for Light Industry (Ministry of Education), Jiangnan University, Wuxi 214122, China

†E-mail: Louxy@jiangnan.edu.cn

Received Nov. 29, 2021; Revision accepted Dec. 21, 2021; Crosschecked Mar. 4, 2022; Published online Apr. 23, 2022

Abstract: This paper investigates the problem of dynamic output-feedback control for a class of Lipschitz nonlinear systems. First, a continuous-time controller is constructed and sufficient conditions for stability of the nonlinear systems are presented. Then, a novel event-triggered mechanism is proposed for the Lipschitz nonlinear systems in which new event-triggered conditions are introduced. Consequently, a closed-loop hybrid system is obtained using the event-triggered control strategy. Sufficient conditions for stability of the closed-loop system are established in the framework of hybrid systems. In addition, an upper bound of a minimum inter-event interval is provided to avoid the Zeno phenomenon. Finally, numerical examples of a neural network system and a genetic regulatory network system are provided to verify the theoretical results and to show the superiority of the proposed method.

Key words: Lipschitz nonlinear system; Dynamic output-feedback control; Event-triggered control; Global asymptotic stability

https://doi.org/10.1631/FITEE.2100552 **CLC number:** TP13

1 Introduction

Nonlinear systems have received much attention for decades due to their broad requirements in scientific and engineering fields such as electrical circuits, chemical processes, and biomedical engineering (Casey et al., 2006; Angulo et al., 2019; Chen J et al., 2019). However, due to the complexity of nonlinear systems, their analysis is still a challenging topic. Specifically, different from linear systems, nonlinear systems must find a suitable real-time solution, even though there may be many such solutions or none (Collins et al., 2006). Note that nonlinear systems with Lipschitz characteristics can avoid this problem, because the local Lipschitz property of the system dynamics ensures local existence and uniqueness of the solution, and even guarantees global existence and uniqueness with some extra conditions (Khalil, 2014). Indeed, nonlinear systems with Lipschitz characteristics are in wide demand in the field of system modeling. For instance, Rehan et al. (2018) presented a class of one-sided Lipschitz nonlinear multi-agent systems that combine linear and Lipschitz nonlinear features and have many applications in synchronization, formation, flocking, and so on. In addition, multi-agent systems with Lipschitz conditions have been studied (Zhang Z et al., 2020) owing to their potential applications in many areas, including autonomous underwater vehicles and distributed sensor networks. Pham et al. (2019) concerned a class of nonlinear Lipschitz systems applied to a real electro-rheological (ER) automotive suspension. Therefore, the analysis of nonlinear systems with Lipschitz characteristics is

‡ Corresponding author

* Project supported by the Jiangsu Provincial Natural Science Foundation of China (No. BK20201340), the 333 High-level Talents Training Project of Jiangsu Province, and the China Postdoctoral Science Foundation (No. 2018M642160)

ORCID: Zhiqian LIU, https://orcid.org/0000-0003-3302-6840; Xuyang LOU, https://orcid.org/0000-0002-7499-1308

meaningful and general.

Among the analyses of nonlinear systems with Lipschitz conditions, the stability issue has attracted significant attention. For the stabilization issue, feedback control as a basic control law has been presented in many applications (e.g., Zuo et al. (2016)). On one hand, state-feedback control, one of the most widely used control methods, has been adopted to solve stability issues by combining some other control strategies (Qian and Lin, 2001; Tabuada, 2007). One of the limitations of this control strategy is that it requires full state measurements, which is often not possible in many scenarios. Therefore, some output-feedback control methods have been established to avoid the full state measurement requirement. Currently, many kinds of output-feedback control strategies exist, such as observer-based output-feedback control, static output-feedback control, and dynamic output-feedback control; see Andrieu and Praly (2009), Zhou et al. (2012), Kammogne et al. (2020), and the references therein. Explicitly, observer-based output-feedback control constructs so-called observers to estimate full states from measured outputs, and uses such estimation to control the system. In Pertew et al. (2006), a Lipschitz observer was introduced and some sufficient conditions were presented for the asymptotic convergence of the closed-loop system. Hamid et al. (2019) considered the design of a regional observer-based controller for the locally Lipschitz nonlinear systems. Note that observer-based output-feedback control still requires that the controlled system is observable. On the other hand, static output-feedback control (Ekramian, 2020) and dynamic output-feedback control do not have such limitations. Moreover, compared with static output-feedback control, the dynamic output-feedback control strategy contains the memory of the output trajectory by introducing the integral of an auxiliary variable and thus leads to better control effects (such as shorter convergence time). Many researchers have devoted effort to the analysis of dynamic output-feedback control for nonlinear systems. For instance, Chen PN et al. (2006) focused on the problem of local stabilization of nonlinear systems by dynamic output-feedback control. Liu W et al. (2016) proposed a dynamic output-feedback control method for fast sampling of discrete-time singularly perturbed systems. Dong and Yang (2008) proposed a dynamic output-feedback controller for continuous-time Takagi–Sugeno (T-S) fuzzy systems. However, to our knowledge, analysis of dynamic output-feedback control for Lipschitz nonlinear systems is still absent.

In this study, we aim to establish dynamic output-feedback control methods for Lipschitz nonlinear systems. Generally speaking, the continuous-time control strategy (Park, 2005; Molaei, 2008) has been widely used to stabilize nonlinear systems and it always guarantees a better control effect than discontinuous strategies. Therefore, we first introduce a continuous-time dynamic output-feedback control law that can stabilize Lipschitz nonlinear systems under certain conditions. However, in many scenarios, Lipschitz nonlinear systems may be networked and large-scale, and may suffer from communication and control resource limitations. In such cases, the proposed continuous-time dynamic output-feedback control is not applicable; hence, an alternative strategy, namely the event-triggered control, is often considered to get rid of communication and control resource constraints. More explicitly, event-triggered control allows considerable reduction of resource usage while guaranteeing the stability and maintaining a certain level of control performance by determining event-triggered conditions accordingly (e.g., Goebel et al. (2012), Yu and Antsaklis (2013), Peng and Yang (2013), Zhang JH and Feng (2014), Zhang XM and Han (2016), Gu et al. (2018), and Shu and Zhai (2020)). Note that event-triggered control involves the control updating problem; that is, the event-triggered control system is a hybrid system with both continuous-time and discrete-time dynamics. Research on stability and stabilization of nonlinear systems using event-triggered control is thus challenging and has received much attention in recent years (Donkers and Heemels, 2012; Abdelrahim et al., 2016; Liu S et al., 2017; Zhang XM and Han, 2017; Theodosis and Dimarogonas, 2019). Specifically, in Theodosis and Dimarogonas (2019), the problems of event-triggered and self-triggered control of nonlinear systems were addressed. The authors exploited certain stability assumptions for the continuous-time system as well as the Lipschitz properties of system dynamics, and presented a strategy to guarantee the stability of the system. Liu S et al. (2017) addressed an event-triggered dynamic output-feedback robust model predictive control strategy, but for a class of discrete polytonic systems rather than nonlinear systems with Lipschitz continuous-time conditions. Donkers and Heemels (2012) studied an event-triggered mechanism which includes a dynamic output-feedback controller. While the system considered in Donkers and Heemels (2012) is a linear system, the controller adopts a simplified form of dynamic output feedback, where the controller reflects only the effect of the integral of the output rather than the usual dynamic output-feedback controller in the form of proportional-integral control. Moreover, the event-triggered condition in Donkers and Heemels (2012) was designed based on the networked output and input signals. Hence, to reduce the number of event-triggered times further, our goal is to establish a new event-triggered condition based on the output and a timer variable.

Motivated by the above results, in this study, we establish an event-triggered dynamic output-feedback controller, under which the hybrid system obtained from a Lipschitz nonlinear system is globally asymptotically stable. In summary, the main contributions are as follows:

1. A continuous-time dynamic output-feedback controller is designed for the considered Lipschitz nonlinear system, to ensure the global asymptotic stability of the closed-loop system.

2. We establish an event-triggered dynamic output-feedback controller with some event-triggered conditions and an upper bound of the minimum inter-event interval. Moreover, by means of hybrid system theory, the obtained closed-loop system is proven to be globally asymptotically stable.

Notions and notations used throughout the paper are as follows: Denote $\mathbb{R}^n$ as the n-dimensional Euclidean space. Denote $\mathbb{R}_{\geq 0}$ as the set of non-negative real numbers, i.e., $\mathbb{R}_{\geq 0} := [0, +\infty)$. Denote $\mathbb{N}$ as the set of natural numbers, i.e., $\mathbb{N} := \{0, 1, \ldots\}$. Given a vector $\boldsymbol{x} \in \mathbb{R}^n$, $\|\boldsymbol{x}\|$ denotes the Euclidean norm. In addition, the distance between a vector $\boldsymbol{x}$ and a subset $\mathcal{A} \subseteq \mathbb{R}^n$ is denoted by $\|\boldsymbol{x}\|_{\mathcal{A}} := \inf\{\|\boldsymbol{x} - \boldsymbol{y}\| : \boldsymbol{y} \in \mathcal{A}\}$. Given a continuously differentiable function $h : \mathbb{R}^n \to \mathbb{R}$ and a function $f : \mathbb{R}^n \to \mathbb{R}^n$, the Lie derivative of h at $\boldsymbol{x}$ in the direction of f is denoted by $\langle \nabla h(\boldsymbol{x}), f(\boldsymbol{x}) \rangle$. Denote $\boldsymbol{A}^{-1}$, $\boldsymbol{A}^{\mathrm{T}}$, and $\lambda(\boldsymbol{A})$ as the inverse, transpose, and eigenvalues of any square matrix $\boldsymbol{A}$, respectively. Let $\boldsymbol{A} > 0$ ($\boldsymbol{A} < 0$) represent that matrix $\boldsymbol{A}$ is positive definite (negative definite). Given a set of square matrices $\{\boldsymbol{A}_1, \boldsymbol{A}_2, \ldots, \boldsymbol{A}_n\}$, we denote $\operatorname{diag}(\boldsymbol{A}_1, \boldsymbol{A}_2, \ldots, \boldsymbol{A}_n) = \begin{bmatrix} \boldsymbol{A}_1 & \ldots & \boldsymbol{0} \\ \vdots & \ddots & \vdots \\ \boldsymbol{0} & \ldots & \boldsymbol{A}_n \end{bmatrix}$. Given a set of vectors $\{\boldsymbol{x}_1, \boldsymbol{x}_2, \ldots, \boldsymbol{x}_m\}$, we denote $\operatorname{col}(\boldsymbol{x}_1, \boldsymbol{x}_2, \ldots, \boldsymbol{x}_m) = [\boldsymbol{x}_1^{\mathrm{T}}, \boldsymbol{x}_2^{\mathrm{T}}, \ldots, \boldsymbol{x}_m^{\mathrm{T}}]^{\mathrm{T}}$. Given matrices $\boldsymbol{A}$, $\boldsymbol{B}$, and $\boldsymbol{C}$ of appropriate dimensions, $\begin{bmatrix} \boldsymbol{A} & \boldsymbol{B} \\ * & \boldsymbol{C} \end{bmatrix}$ denotes $\begin{bmatrix} \boldsymbol{A} & \boldsymbol{B} \\ \boldsymbol{B}^{\mathrm{T}} & \boldsymbol{C} \end{bmatrix}$. A function $\alpha : \mathbb{R}_{\geq 0} \to \mathbb{R}_{\geq 0}$ belongs to class $\mathcal{K}$ if it is zero at zero, continuous, and strictly increasing; it belongs to class $\mathcal{K}_\infty$ if, in addition, is unbounded. A function $\rho : \mathbb{R}_{\geq 0} \to \mathbb{R}_{\geq 0}$ belongs to $\mathcal{PD}$ (positive definite) if it is continuous; $\rho(s) > 0$ for all $s > 0$, and $\rho(s) = 0$ for $s = 0$.

2 Preliminary results and problem formulation

Consider a class of nonlinear control systems as follows:

$$\begin{aligned} \dot{\boldsymbol{x}} &= \boldsymbol{A}\boldsymbol{x} + \boldsymbol{B}f(\boldsymbol{x}) + \boldsymbol{E}\boldsymbol{u}, \\ \boldsymbol{y} &= \boldsymbol{C}\boldsymbol{x}, \end{aligned} \tag{1}$$

where $\boldsymbol{x} \in \mathbb{R}^{n_x}$ denotes the state vector, $\boldsymbol{u} \in \mathbb{R}^{n_u}$ the input, and $\boldsymbol{y} \in \mathbb{R}^{n_y}$ the output. Matrices $\boldsymbol{A}$, $\boldsymbol{B}$, $\boldsymbol{C}$, and $\boldsymbol{E}$ are real matrices of appropriate dimensions. In addition, the function $f(\boldsymbol{x}) = [f_1(\boldsymbol{x}), f_2(\boldsymbol{x}), \ldots, f_{n_x}(\boldsymbol{x})]^{\mathrm{T}}$ is the nonlinear part such that for each i ($i = 1, 2, \ldots, n_x$), the following so-called Lipschitz conditions (Zhang Z et al., 2020) hold:

1. $f_i(\boldsymbol{0}) = \boldsymbol{0}$;

2. There exist constant numbers $l_i > 0$ satisfying $\|f_i(\boldsymbol{m}(t)) - f_i(\boldsymbol{n}(t))\| \leq l_i \|\boldsymbol{m}(t) - \boldsymbol{n}(t)\|$ for any $\boldsymbol{m}(t), \boldsymbol{n}(t) \in \mathbb{R}^{n_x}$.

It follows immediately from the above conditions that system (1) has at least one equilibrium $\boldsymbol{x}^* = \boldsymbol{0}$. However, in general, the equilibrium of system (1) may not be globally asymptotically stable. Therefore, we aim to find some suitable $\boldsymbol{u}$ to guarantee the global asymptotic stability of system (1) at $\boldsymbol{x}^*$. In addition, in many scenarios, some entries of $\boldsymbol{x}$ cannot be controlled; i.e., some rows of $\boldsymbol{E}$ have all "0" elements. Without loss of generality, we assume that $\boldsymbol{E} = [\boldsymbol{0} \quad \boldsymbol{I}]^{\mathrm{T}}$, where $\boldsymbol{0}$ represents a zero matrix of appropriate dimensions and $\boldsymbol{I}$ represents an identity matrix of appropriate dimensions. Correspondingly, we partition matrices $\boldsymbol{A}$, $\boldsymbol{B}$, and

$\boldsymbol{C}$ as $\boldsymbol{A} = \begin{bmatrix} \boldsymbol{A}_1 & \boldsymbol{A}_2 \\ \boldsymbol{A}_3 & \boldsymbol{A}_4 \end{bmatrix}$, $\boldsymbol{B} = \begin{bmatrix} \boldsymbol{B}_1 & \boldsymbol{B}_2 \\ \boldsymbol{B}_3 & \boldsymbol{B}_4 \end{bmatrix}$, and $\boldsymbol{C} = [\boldsymbol{C}_1 \ \ \boldsymbol{C}_2]$, respectively. Meanwhile, the Lipschitz condition of function f is given by the following statement: there exists a positive definite matrix $\boldsymbol{M}$ such that

$$\begin{aligned}&\left(f(\boldsymbol{x}) - f(\boldsymbol{x}^*)\right)^{\mathrm{T}} \boldsymbol{M} \left(f(\boldsymbol{x}) - f(\boldsymbol{x}^*)\right) \\ \leq& (\boldsymbol{x} - \boldsymbol{x}^*)^{\mathrm{T}} \boldsymbol{L}^{\mathrm{T}} \boldsymbol{M} \boldsymbol{L} (\boldsymbol{x} - \boldsymbol{x}^*), \ \forall \boldsymbol{x} \in \mathbb{R}^{n_x},\end{aligned} \tag{2}$$

where $\boldsymbol{L} = \operatorname{diag}(l_1, l_2, \ldots, l_{n_x})$, and $\boldsymbol{L}$ can also be partitioned as $\boldsymbol{L} = \begin{bmatrix} \boldsymbol{L}_1 & \boldsymbol{0} \\ * & \boldsymbol{L}_2 \end{bmatrix}$ comparable to the dimensions of $\boldsymbol{u}$. Hence, the control object in this study is to design suitable output-feedback controllers such that the obtained closed-loop system is globally asymptotically stable.

More explicitly, we will design the following dynamic output-feedback controller:

$$\begin{aligned}\dot{\boldsymbol{\xi}} &= \boldsymbol{A}_{\mathrm{c}} \boldsymbol{\xi} + \boldsymbol{B}_{\mathrm{c}} \boldsymbol{y}, \\ \boldsymbol{u} &= \boldsymbol{C}_{\mathrm{c}} \boldsymbol{\xi} + \boldsymbol{D}_{\mathrm{c}} \boldsymbol{y},\end{aligned} \tag{3}$$

where $\boldsymbol{\xi} \in \mathbb{R}^{n_\xi}$ is the state of the controller, and matrices $\boldsymbol{A}_{\mathrm{c}}$, $\boldsymbol{B}_{\mathrm{c}}$, $\boldsymbol{C}_{\mathrm{c}}$, and $\boldsymbol{D}_{\mathrm{c}}$ are of comparable dimensions and will be determined later. Combining Eqs. (1) and (3), we obtain the following closed-loop system:

$$\begin{aligned}\dot{\boldsymbol{x}} &= (\boldsymbol{A} + \boldsymbol{E} \boldsymbol{D}_{\mathrm{c}} \boldsymbol{C}) \boldsymbol{x} + \boldsymbol{B} f(\boldsymbol{x}) + \boldsymbol{E} \boldsymbol{C}_{\mathrm{c}} \boldsymbol{\xi}, \\ \dot{\boldsymbol{\xi}} &= \boldsymbol{A}_{\mathrm{c}} \boldsymbol{\xi} + \boldsymbol{B}_{\mathrm{c}} \boldsymbol{C} \boldsymbol{x}.\end{aligned} \tag{4}$$

Next, we will provide conditions under which the above closed-loop system (4) is globally asymptotically stable.

Theorem 1 Consider system (1) under controller (3). Suppose that there exist positive definite matrices $\boldsymbol{X}_1$, $\boldsymbol{X}_2$, $\boldsymbol{Q}_1$, $\boldsymbol{Q}_2$ and real matrices $\bar{\boldsymbol{A}}_{\mathrm{c}}$, $\bar{\boldsymbol{B}}_{\mathrm{c}}$, $\bar{\boldsymbol{C}}_{\mathrm{c}}$, $\bar{\boldsymbol{D}}_{\mathrm{c}}$ of appropriate dimensions satisfying

$$\begin{bmatrix} \boldsymbol{\omega}_{11} & \boldsymbol{\omega}_{12} & \boldsymbol{C}_1^{\mathrm{T}} \bar{\boldsymbol{B}}_{\mathrm{c}}^{\mathrm{T}} & \boldsymbol{X}_1 \boldsymbol{B}_1 & \boldsymbol{X}_1 \boldsymbol{B}_2 \\ * & \boldsymbol{\omega}_{22} & \bar{\boldsymbol{C}}_{\mathrm{c}} + \boldsymbol{C}_2^{\mathrm{T}} \bar{\boldsymbol{B}}_{\mathrm{c}}^{\mathrm{T}} & \boldsymbol{X}_2 \boldsymbol{B}_3 & \boldsymbol{X}_2 \boldsymbol{B}_4 \\ * & * & \bar{\boldsymbol{A}}_{\mathrm{c}}^{\mathrm{T}} + \bar{\boldsymbol{A}}_{\mathrm{c}} & \boldsymbol{0} & \boldsymbol{0} \\ * & * & * & -\boldsymbol{Q}_1 & \boldsymbol{0} \\ * & * & * & * & -\boldsymbol{Q}_2 \end{bmatrix} < 0, \tag{5}$$

where $\boldsymbol{\omega}_{11} = \boldsymbol{A}_1^{\mathrm{T}} \boldsymbol{X}_1 + \boldsymbol{X}_1 \boldsymbol{A}_1 + \boldsymbol{L}_1 \boldsymbol{Q}_1 \boldsymbol{L}_1$, $\boldsymbol{\omega}_{12} = \boldsymbol{A}_3^{\mathrm{T}} \boldsymbol{X}_2 + \boldsymbol{C}_1^{\mathrm{T}} \bar{\boldsymbol{D}}_{\mathrm{c}}^{\mathrm{T}} + \boldsymbol{X}_1 \boldsymbol{A}_2$, and $\boldsymbol{\omega}_{22} = \boldsymbol{A}_4^{\mathrm{T}} \boldsymbol{X}_2 + \boldsymbol{C}_2^{\mathrm{T}} \bar{\boldsymbol{D}}_{\mathrm{c}}^{\mathrm{T}} + \boldsymbol{X}_2 \boldsymbol{A}_4 + \bar{\boldsymbol{D}}_{\mathrm{c}} \boldsymbol{C}_2 + \boldsymbol{L}_2 \boldsymbol{Q}_2 \boldsymbol{L}_2$.

Let the gains of controller (3) be given by

$$\begin{aligned}&\boldsymbol{A}_{\mathrm{c}} = q \bar{\boldsymbol{A}}_{\mathrm{c}}, \ \ \boldsymbol{B}_{\mathrm{c}} = q \bar{\boldsymbol{B}}_{\mathrm{c}}, \\ &\boldsymbol{C}_{\mathrm{c}} = \bar{\boldsymbol{X}}_2^{-1} \bar{\boldsymbol{C}}_{\mathrm{c}}, \ \ \boldsymbol{D}_{\mathrm{c}} = \bar{\boldsymbol{X}}_2^{-1} \bar{\boldsymbol{D}}_{\mathrm{c}},\end{aligned} \tag{6}$$

where q is a positive constant. Then, we have that closed-loop system (4) is globally asymptotically stable.

The proof of the above theorem can be found in Appendix.

Remark 1 Theorem 1 is given to establish sufficient conditions for the closed-loop system under continuous-time dynamic output-feedback control. In fact, it is also a new result compared to the literature related to the control of Lipschitz nonlinear systems.

Up to now, we have established conditions for the asymptotic stability of system (4) under continuous-time dynamic output-feedback control. Although continuous-time control performs well, in many scenarios, nonlinear systems may have limited communication and control resources because of their large-scale and underlying interconnection networks. To get rid of this obstacle, one needs to adopt other control strategies. Specifically, in the following, we will consider the so-called event-triggered control strategy to improve the communication efficiency. Moreover, event-triggered control allows considerable reduction of resource usage while guaranteeing stability and maintaining a certain level of control performance by determining event-triggered conditions accordingly (Peng and Yang, 2013). Hence, compared with the continuous-time control method, event-triggered control is more feasible and practical in many system applications. According to this kind of control strategy, one first provides event-triggered conditions and then uses the event detector to continuously monitor the event-triggered conditions to determine whether an "event" occurs or not. Once an event occurs, the event detector will transmit the newest output measurement to the event-triggered controller. Specifically, denote the time instants when an event occurs by a sequence

$$t_0, \ t_1, \ t_2, \ \cdots.$$

Consequently, we will obtain a set of measured outputs $\{\boldsymbol{y}(t_k)\}_{k=0}^{\infty}$. To ensure continuous injection of the signal into the controller, the zero-order holder (ZOH) mechanism is adopted to generate the continuous-time signal:

$$\bar{\boldsymbol{y}}(t) = \boldsymbol{y}(t_k), \ t_k \leq t < t_{k+1}.$$

In summary, the schematic of the above event-triggered dynamic output-feedback control is depicted in Fig. 1b with the continuous-time control method depicted in Fig. 1a.

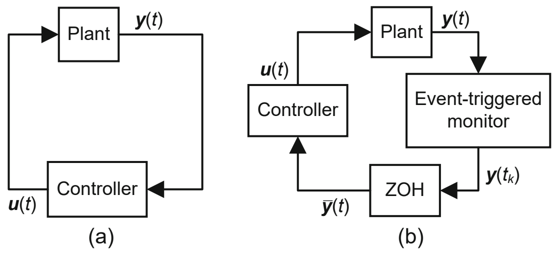

Fig. 1 Continuous-time (a) and event-triggered (b) dynamic output-feedback control schematics (ZOH: zero-order holder)

Define the measurement error as $\boldsymbol{e}(t) := \bar{\boldsymbol{y}}(t) - \boldsymbol{y}(t)$ for $t \geq 0$; hence, the closed-loop event-triggered system can be written as

$$\begin{aligned} \dot{\boldsymbol{x}} &= (\boldsymbol{A} + \boldsymbol{E}\boldsymbol{D}_{\mathrm{c}}\boldsymbol{C})\,\boldsymbol{x} + \boldsymbol{B}f(\boldsymbol{x}) + \boldsymbol{E}\boldsymbol{C}_{\mathrm{c}}\boldsymbol{\xi} + \boldsymbol{E}\boldsymbol{D}_{\mathrm{c}}\boldsymbol{e}, \\ \dot{\boldsymbol{\xi}} &= \boldsymbol{A}_{\mathrm{c}}\boldsymbol{\xi} + \boldsymbol{B}_{\mathrm{c}}\boldsymbol{e} + \boldsymbol{B}_{\mathrm{c}}\boldsymbol{C}\boldsymbol{x}. \end{aligned} \tag{7}$$

Moreover, for $k \in \mathbb{N}$, we have

$$\begin{aligned} &\dot{\boldsymbol{e}}(t) = -\boldsymbol{C}\dot{\boldsymbol{x}}(t),\ t \in (t_k, t_{k+1}), \\ &\boldsymbol{e}^{+}(t) = \boldsymbol{0},\ t = t_k. \end{aligned}$$

For the sake of simplicity, we introduce the following notions:

$$\begin{aligned} &\boldsymbol{\zeta} := \mathrm{col}\,(\boldsymbol{x}, \boldsymbol{\xi}), \\ &f_a(\boldsymbol{\zeta}, \boldsymbol{e}) = \begin{bmatrix} \boldsymbol{A} + \boldsymbol{E}\boldsymbol{D}_{\mathrm{c}}\boldsymbol{C} & \boldsymbol{E}\boldsymbol{C}_{\mathrm{c}} \\ \boldsymbol{B}_{\mathrm{c}}\boldsymbol{C} & \boldsymbol{A}_{\mathrm{c}} \end{bmatrix} \boldsymbol{\zeta} + \begin{bmatrix} \boldsymbol{B} \\ \boldsymbol{0} \end{bmatrix} g(\boldsymbol{\zeta}) + \begin{bmatrix} \boldsymbol{E}\boldsymbol{D}_{\mathrm{c}} \\ \boldsymbol{B}_{\mathrm{c}} \end{bmatrix} \boldsymbol{e}, \\ &f_b\,(\boldsymbol{\zeta}, \boldsymbol{e}) \\ &= -\boldsymbol{C}\left([\boldsymbol{A} + \boldsymbol{E}\boldsymbol{D}_{\mathrm{c}}\boldsymbol{C} \quad \boldsymbol{E}\boldsymbol{C}_{\mathrm{c}}]\boldsymbol{\zeta} + \boldsymbol{B}g(\boldsymbol{\zeta}) + \boldsymbol{E}\boldsymbol{D}_{\mathrm{c}}\boldsymbol{e}\right), \end{aligned}$$

where $g(\boldsymbol{\zeta}) = f(\boldsymbol{x})$. Consequently, the hybrid system is obtained as

$$\mathcal{H}: \begin{array}{l} \begin{cases} \dot{\boldsymbol{\zeta}} = f_a\,(\boldsymbol{\zeta}, \boldsymbol{e}) \\ \dot{\boldsymbol{e}} = f_b\,(\boldsymbol{\zeta}, \boldsymbol{e}) & (\boldsymbol{\zeta}, \boldsymbol{e}, \tau) \in \mathcal{F}, \\ \dot{\tau} = 1 \end{cases} \\ \begin{cases} \boldsymbol{\zeta}^{+} = \boldsymbol{\zeta} \\ \boldsymbol{e}^{+} = \boldsymbol{0} & (\boldsymbol{\zeta}, \boldsymbol{e}, \tau) \in \mathcal{J}, \\ \tau^{+} = 0 \end{cases} \end{array} \tag{8}$$

where $\tau \geq 0$ is a timer variable introduced to reduce the event frequency. For the sake of notation simplicity, we define

$$F\,(\boldsymbol{\zeta}, \boldsymbol{e}, \tau) = \begin{bmatrix} f_a(\boldsymbol{\zeta}, \boldsymbol{e}) \\ f_b(\boldsymbol{\zeta}, \boldsymbol{e}) \\ 1 \end{bmatrix},\ G\,(\boldsymbol{\zeta}, \boldsymbol{e}, \tau) = \begin{bmatrix} \boldsymbol{\zeta} \\ \boldsymbol{0} \\ 0 \end{bmatrix}.$$

In the sequel, a hybrid system defined as above will be represented by the notation $\mathcal{H} = (F, \mathcal{F}, G, \mathcal{J})$, or briefly, $\mathcal{H}$.

In event-triggered control, transmissions occur whenever the event-triggered conditions are satisfied. Hybrid model (8) is well-equipped to describe dynamic systems with event-triggered control. Indeed, a transmission can be modeled as a jump of system (8) that will be generated whenever the event-triggered condition is satisfied. This indicates that the state of system (8) enters in $\mathcal{J}$ at the transmission instant. When events are not generated, it means that the state of system (8) is in $\mathcal{F}$, and the system evolves along with flows.

To conclude this section, we formally state the research problem of this study as follows:

Problem statement Consider the hybrid system $\mathcal{H} = (F, \mathcal{F}, G, \mathcal{J})$ given by Eq. (8). Our goal is to design the flow map F, jump map G, flow set $\mathcal{F}$, and jump set $\mathcal{J}$ to guarantee that the hybrid system $\mathcal{H}$ is uniformly globally asymptotically stable.

3 Main results

In this section, recalling the hybrid system $\mathcal{H} = (F, \mathcal{F}, G, \mathcal{J})$ in Eq. (8), we will first design the controller gains $\boldsymbol{A}_{\mathrm{c}}$, $\boldsymbol{B}_{\mathrm{c}}$, $\boldsymbol{C}_{\mathrm{c}}$, and $\boldsymbol{D}_{\mathrm{c}}$ and the event-triggered conditions. Second, based on the design of the controller and event-triggered conditions, we separately determine the flow map F, jump map G, flow set $\mathcal{F}$, and jump set $\mathcal{J}$ for the hybrid system $\mathcal{H}$. Moreover, we establish the stability criterion under which the obtained closed-loop hybrid system is globally asymptotically stable by the hybrid system theory without the Zeno phenomenon.

Before presenting the main results, some preliminaries and concepts related to the framework for stability analysis of hybrid systems will be reviewed first, following the conventions (Nesic et al., 2009; Goebel et al., 2012; Meslem and Prieur, 2015).

A set $\varepsilon \subseteq \mathbb{R}_{\geq 0} \times \mathbb{N}$ is called a compact hybrid time domain if for some finite time sequence $0 = t_0 \leq t_1 \leq \ldots \leq t_J$, there is $\varepsilon = \cup_{j=0}^{J-1}\,([t_j, t_{j+1}], j)$. We further call ε a hybrid time domain, if for all

$(T,J)\in\varepsilon$, $\varepsilon\cap([0,T]\times\{0,1,\ldots,J\})$ is a compact hybrid time domain. Moreover, a hybrid trajectory is a pair (dom $\boldsymbol{z},\boldsymbol{z}$) consisting of a hybrid time domain dom $\boldsymbol{z}$ and a function $\boldsymbol{z}$ defined on dom $\boldsymbol{z}$ that is continuously differentiable in t on (dom $\boldsymbol{z})\cap(\mathbb{R}_{\geq 0}\times\{0,1,\ldots\})$. In addition, for the hybrid system $\mathcal{H}$ given by the open set $O\in\mathbb{R}^n$ and the data $(F,\mathcal{F},G,\mathcal{J})$ where $F:O\to\mathbb{R}^n$ is continuous, $G:O\to O$ is locally bounded, and $\mathcal{F}$ and $\mathcal{J}$ are subsets of O, we say that a hybrid trajectory $\boldsymbol{z}$: dom $\boldsymbol{z}\to O$ is a solution to $\mathcal{H}$ if the following conditions hold:

1. For all $j\in\mathbb{N}$ and for almost all $t\in I_j$, where I_j is such that $I_j\times\{j\}:=\text{dom}\,\boldsymbol{z}\cap(\mathbb{R}_{\geq 0}\times\{j\})$, we have $\boldsymbol{z}(t,j)\in\mathcal{F}$ and $\dot{\boldsymbol{z}}(t,j)=F(\boldsymbol{z}(t,j))$.

2. For all $(t,j)\in$ dom $\boldsymbol{z}$ such that $(t,j+1)\in$ dom $\boldsymbol{z}$, we have $\boldsymbol{z}(t,j)\in\mathcal{J}$ and $\boldsymbol{z}(t,j+1)=G(\boldsymbol{z}(t,j))$.

Then, we have the following definition for analyzing the stability of hybrid system (8):

Definition 1 For hybrid system (8), the set $\mathcal{A}=\{(\boldsymbol{\zeta},\boldsymbol{e},\tau):\boldsymbol{\zeta}=\mathbf{0},\ \boldsymbol{e}=\mathbf{0},\ \tau\in\mathbb{R}_{\geq 0}\}$ is uniformly globally pre-asymptotically stable, if the following properties hold:

1. Uniform global stability

There exists a function $\alpha:\mathbb{R}_{\geq 0}\to\mathbb{R}_{\geq 0}$ belonging to class $\mathcal{K}_\infty$ such that for any solution $\boldsymbol{z}(t,j)$ to system (8), $\|\boldsymbol{z}(t,j)\|_{\mathcal{A}}<\alpha(\|\boldsymbol{z}(0,0)\|_{\mathcal{A}})$ for all $(t,j)\in$ dom $\boldsymbol{z}$.

2. Uniform global pre-attractivity

For each ε, $r>0$, there exists a positive real number T such that for any solution $\boldsymbol{z}(t,j)$ to system (8) with $\|\boldsymbol{z}(0,0)\|_{\mathcal{A}}<r$, $(t,j)\in$ dom $\boldsymbol{z}$ and $t+j\geq T$ imply $\|\boldsymbol{z}(t,j)\|_{\mathcal{A}}<\varepsilon$, and $\mathcal{A}$ is said to be uniformly globally asymptotically stable (UGAS) when, in addition, the maximal solutions to system (8) are complete.

Furthermore, a function V: dom $V\to\mathbb{R}$ is said to be a Lyapunov function candidate for the hybrid system $\mathcal{H}=(F,\mathcal{F},G,\mathcal{J})$ if the following conditions hold:

1. $\bar{\mathcal{F}}\cup\mathcal{J}\cup G(\mathcal{J})\subset$ dom V;

2. V is continuously differentiable on an open set containing $\bar{\mathcal{F}}$, where $\bar{\mathcal{F}}$ denotes the closure of $\mathcal{F}$.

Based on the aforementioned notions, we can introduce the following condition, under which a given closed set $\mathcal{A}$ is UGAS for system $\mathcal{H}$:

Lemma 1 (Goebel et al. (2012), Proposition 3.27) Consider a hybrid system $\mathcal{H}=(F,\mathcal{F},G,\mathcal{J})$ and a closed set $\mathcal{A}\subseteq\mathbb{R}^n$. Suppose that V is a Lyapunov function candidate for $\mathcal{H}$ and there exist α_1, $\alpha_2\in\mathcal{K}_\infty$ and $\rho\in\mathcal{PD}$ such that the following inequalities hold:

$$\alpha_1(\|\boldsymbol{z}\|_{\mathcal{A}})\leq V(\boldsymbol{z})\leq\alpha_2(\|\boldsymbol{z}\|_{\mathcal{A}}),\ \forall\boldsymbol{z}\in\mathcal{F}\cup\mathcal{J}\cup G(\mathcal{J}),\tag{9}$$

$$V(g)-V(\boldsymbol{z})\leq 0,\ \forall\boldsymbol{z}\in\mathcal{J},\ g\in G(\boldsymbol{z}),\tag{10}$$

$$\langle\nabla V(\boldsymbol{z}),f\rangle\leq-\rho(\|\boldsymbol{z}\|_{\mathcal{A}}),\boldsymbol{z}\in\mathcal{F},f\in F(\boldsymbol{z}).\tag{11}$$

If for each $r>0$, there exist $\gamma_r\in\mathcal{K}_\infty$ and $N_r\geq 0$ such that for every solution $\boldsymbol{z}$ to $\mathcal{H}$, $\|\boldsymbol{z}(0,0)\|_{\mathcal{A}}\in(0,r]$, $(t,j)\in$ dom $\boldsymbol{z}$, and $t+j\geq T$ imply that $t\geq\gamma_r(T)-N_r$, then $\mathcal{A}$ is uniformly globally pre-asymptotically stable for $\mathcal{H}$.

We recall the following lemmas, which will be used to prove the primary theorem next:

Lemma 2 (Qiu (2007), Lemma 3) For any vectors $\boldsymbol{x}$ and $\boldsymbol{y}$ with appropriate dimensions, the inequality $2\boldsymbol{x}^{\mathrm{T}}\boldsymbol{y}\leq\boldsymbol{x}^{\mathrm{T}}\boldsymbol{\Sigma}\boldsymbol{x}+\boldsymbol{y}^{\mathrm{T}}\boldsymbol{\Sigma}_3^{-1}\boldsymbol{y}$ holds, in which $\boldsymbol{\Sigma}$ is any matrix with $\boldsymbol{\Sigma}>0$.

Lemma 3 (Wang et al. (2002), Lemma 1) Given symmetric matrices $\boldsymbol{\Sigma}_1$, $\boldsymbol{\Sigma}_2$, $\boldsymbol{\Sigma}_3$ with $\boldsymbol{\Sigma}_2>0$, then $\boldsymbol{\Sigma}_1+\boldsymbol{\Sigma}_3^{\mathrm{T}}\boldsymbol{\Sigma}_2^{-1}\boldsymbol{\Sigma}_3<0$ if and only if $\begin{bmatrix}\boldsymbol{\Sigma}_1 & \boldsymbol{\Sigma}_3^{\mathrm{T}}\\ \boldsymbol{\Sigma}_3 & -\boldsymbol{\Sigma}_2\end{bmatrix}<0$ or $\begin{bmatrix}-\boldsymbol{\Sigma}_2 & \boldsymbol{\Sigma}_3\\ \boldsymbol{\Sigma}_3^{\mathrm{T}} & \boldsymbol{\Sigma}_1\end{bmatrix}<0$.

We now move on to the design of the output-feedback controller with controller gains defined as

$$\begin{aligned}\boldsymbol{A}_{\mathrm{c}}=\tilde{\boldsymbol{X}}_1\tilde{\boldsymbol{A}}_{\mathrm{c}},\ \boldsymbol{B}_{\mathrm{c}}=\tilde{\boldsymbol{X}}_1\tilde{\boldsymbol{B}}_{\mathrm{c}},\\ \boldsymbol{C}_{\mathrm{c}}=\tilde{\boldsymbol{X}}_2\tilde{\boldsymbol{C}}_{\mathrm{c}},\ \boldsymbol{D}_{\mathrm{c}}=\tilde{\boldsymbol{X}}_2\tilde{\boldsymbol{D}}_{\mathrm{c}},\end{aligned}$$

where $\tilde{\boldsymbol{X}}_1$ and $\tilde{\boldsymbol{X}}_2$ are positive definite matrices, and $\tilde{\boldsymbol{A}}_{\mathrm{c}}$, $\tilde{\boldsymbol{B}}_{\mathrm{c}}$, $\tilde{\boldsymbol{C}}_{\mathrm{c}}$, and $\tilde{\boldsymbol{D}}_{\mathrm{c}}$ are nonzero matrices. Accordingly, the flow map F and jump map G in system (8) can be determined immediately as

$$F(\boldsymbol{\zeta},\boldsymbol{e},\tau)=\begin{bmatrix}\tilde{f}_a(\boldsymbol{\zeta},\boldsymbol{e})\\ \tilde{f}_b(\boldsymbol{\zeta},\boldsymbol{e})\\ \tilde{f}_c(\tau)\end{bmatrix},\ G(\boldsymbol{\zeta},\boldsymbol{e},\tau)=\begin{bmatrix}\boldsymbol{\zeta}\\ \mathbf{0}\\ 0\end{bmatrix},\tag{12}$$

where

$$\begin{aligned}\tilde{f}_a(\boldsymbol{\zeta},\boldsymbol{e})=&\begin{bmatrix}\boldsymbol{A}+\boldsymbol{E}\tilde{\boldsymbol{X}}_2\tilde{\boldsymbol{D}}_{\mathrm{c}}\boldsymbol{C} & \boldsymbol{E}\tilde{\boldsymbol{X}}_2\tilde{\boldsymbol{C}}_{\mathrm{c}}\\ \tilde{\boldsymbol{X}}_1\tilde{\boldsymbol{B}}_{\mathrm{c}}\boldsymbol{C} & \tilde{\boldsymbol{X}}_1\tilde{\boldsymbol{A}}_{\mathrm{c}}\end{bmatrix}\boldsymbol{\zeta}\\ &+\begin{bmatrix}\boldsymbol{B}\\ \mathbf{0}\end{bmatrix}g(\boldsymbol{\zeta})+\begin{bmatrix}\boldsymbol{E}\tilde{\boldsymbol{X}}_2\tilde{\boldsymbol{D}}_{\mathrm{c}}\\ \tilde{\boldsymbol{X}}_1\tilde{\boldsymbol{B}}_{\mathrm{c}}\end{bmatrix}\boldsymbol{e},\end{aligned}$$

$$\begin{aligned}\tilde{f}_b(\boldsymbol{\zeta},\boldsymbol{e}) = & -\boldsymbol{C}\left(\left[\boldsymbol{A}+\boldsymbol{E}\tilde{\boldsymbol{X}}_2\tilde{\boldsymbol{D}}_\mathrm{c}\boldsymbol{C} \quad \boldsymbol{E}\tilde{\boldsymbol{X}}_2\tilde{\boldsymbol{C}}_\mathrm{c}\right]\boldsymbol{\zeta}\right.\\ & \left. +\boldsymbol{B}g(\boldsymbol{\zeta})+\boldsymbol{E}\tilde{\boldsymbol{X}}_2\tilde{\boldsymbol{D}}_\mathrm{c}\boldsymbol{e}\right),\\ \tilde{f}_c(\tau) = & \ 1.\end{aligned}$$

Next, to construct the flow set $\mathcal{F}$ and jump set $\mathcal{J}$, we will introduce the following auxiliary parameter variables:

$$\begin{aligned}\kappa &:= \lambda_{\max}^{-1}(\boldsymbol{\varXi}_1),\\ \gamma &:= \lambda_{\max}(\boldsymbol{\varXi}_1)\lambda_{\max}(\boldsymbol{\varXi}_2),\\ \ell &:= \max\{\lambda_{\max}(\boldsymbol{\varXi}_3), 2\gamma\},\end{aligned}$$

where

$$\begin{aligned}\boldsymbol{\varXi}_1 = & \operatorname{diag}\Big(\boldsymbol{L}\boldsymbol{B}^\mathrm{T}\boldsymbol{C}^\mathrm{T}\boldsymbol{\varPi}_1\boldsymbol{C}\boldsymbol{B}\boldsymbol{L}\\ & + (\boldsymbol{A}+\boldsymbol{E}\boldsymbol{D}_\mathrm{c}\boldsymbol{C})^\mathrm{T}\boldsymbol{C}^\mathrm{T}\boldsymbol{\varPi}_2\boldsymbol{C}(\boldsymbol{A}+\boldsymbol{E}\boldsymbol{D}_\mathrm{c}\boldsymbol{C}),\\ & \boldsymbol{C}_\mathrm{c}^\mathrm{T}\boldsymbol{E}^\mathrm{T}\boldsymbol{C}^\mathrm{T}\boldsymbol{\varPi}_3\boldsymbol{C}\boldsymbol{E}\boldsymbol{C}_\mathrm{c}\Big),\\ \boldsymbol{\varXi}_2 = & \boldsymbol{D}_\mathrm{c}^\mathrm{T}\boldsymbol{E}^\mathrm{T}\boldsymbol{\varPi}_4\boldsymbol{E}\boldsymbol{D}_\mathrm{c}+\boldsymbol{B}_\mathrm{c}^\mathrm{T}\boldsymbol{N}_3\boldsymbol{B}_\mathrm{c},\\ \boldsymbol{\varXi}_3 = & -\boldsymbol{D}_\mathrm{c}^\mathrm{T}\boldsymbol{E}^\mathrm{T}\boldsymbol{C}^\mathrm{T}-\boldsymbol{C}\boldsymbol{E}\boldsymbol{D}_\mathrm{c}+\boldsymbol{\varPi}_1^{-1}+\boldsymbol{\varPi}_2^{-1}+\boldsymbol{\varPi}_3^{-1}.\end{aligned} \tag{13}$$

Here, $\boldsymbol{\varPi}_4 = \operatorname{diag}(\boldsymbol{N}_1,\boldsymbol{N}_2)$, and $\boldsymbol{N}_1$, $\boldsymbol{N}_2$, $\boldsymbol{N}_3$, $\boldsymbol{\varPi}_1$, $\boldsymbol{\varPi}_2$, $\boldsymbol{\varPi}_3$ are positive definite matrices. Consequently, the flow set $\mathcal{F}$ and jump set $\mathcal{J}$ are defined as

$$\begin{aligned}\mathcal{F} &= \{(\boldsymbol{\zeta},\boldsymbol{e},\tau): \gamma U(\boldsymbol{e}) \le \delta(\boldsymbol{y}) \ \text{or} \ \tau\in[0,\bar{\tau}]\},\\ \mathcal{J} &= \{(\boldsymbol{\zeta},\boldsymbol{e},\tau): \gamma U(\boldsymbol{e}) \ge \delta(\boldsymbol{y}) \ \text{and} \ \tau\ge\bar{\tau}\},\end{aligned} \tag{14}$$

where $0 < \bar{\tau} \le \frac{1}{\bar{\ell}}\ln\left(\frac{\gamma-\ell+\bar{\ell}}{\gamma}+\frac{\ell}{\bar{\ell}}\right)$, $\delta(\boldsymbol{y}) = \boldsymbol{y}^\mathrm{T}\tilde{\boldsymbol{X}}_3\boldsymbol{y}$, and $U(\boldsymbol{e}) = \kappa\boldsymbol{e}^\mathrm{T}\boldsymbol{e}$, with $\tilde{\boldsymbol{X}}_3$ being a positive definite matrix and $\bar{\ell}$ a positive constant satisfying $\bar{\ell} > \ell$.

Remark 2 The flow set $\mathcal{F}$ and jump set $\mathcal{J}$ indicate the event-triggered conditions. Note that $\mathcal{F}\cap\mathcal{J} = \{(\boldsymbol{\zeta},\boldsymbol{e},\tau): \gamma U(\boldsymbol{e}) = \delta(\boldsymbol{y}) \text{ and } \tau = \bar{\tau}\} \neq \varnothing$, which implies that when $(\boldsymbol{\zeta},\boldsymbol{e},\tau)\in\mathcal{F}\cap\mathcal{J}$, the evolution of the system may have two possibilities: (1) the solution may flow only if the states $(\boldsymbol{\zeta},\boldsymbol{e},\tau)$ are kept in $\mathcal{F}$; (2) the system experiences a jump, otherwise.

For convenience, let $n = n_x + n_\xi + n_y + 1$. Next, we will establish a sufficient condition under which the above system $\mathcal{H} = (F,\mathcal{F},G,\mathcal{J})$ is globally asymptotically stable for a given closed set $\mathcal{A}\subseteq\mathbb{R}^n$.

Theorem 2 Consider the hybrid system $\mathcal{H} = (F,\mathcal{F},G,\mathcal{J})$ with F,G given in Eq. (12) and $\mathcal{F},\mathcal{J}$ given in Eq. (14), and consider the closed set $\mathcal{A} = \{0\}\times\{0\}\times\mathbb{R}_{\ge 0}\subseteq\mathbb{R}^n$. Suppose that matrices $\tilde{\boldsymbol{X}}_1$, $\tilde{\boldsymbol{X}}_2$, $\tilde{\boldsymbol{X}}_3$, $\boldsymbol{N}_1$, $\boldsymbol{N}_2$, $\boldsymbol{N}_3$, $\tilde{\boldsymbol{A}}_\mathrm{c}$, $\tilde{\boldsymbol{B}}_\mathrm{c}$, $\tilde{\boldsymbol{C}}_\mathrm{c}$, and $\tilde{\boldsymbol{D}}_\mathrm{c}$ in Eqs. (12) and (14) satisfy linear matrix inequality (LMI) (15) (on top of the next page).

In LMI (15), $\bar{\boldsymbol{X}}_1 = \tilde{\boldsymbol{X}}_1^{-1}$, $\bar{\boldsymbol{X}}_2 = \tilde{\boldsymbol{X}}_2^{-1}$, $\bar{\boldsymbol{X}}_3 = \tilde{\boldsymbol{X}}_3^{-1}$, $\tilde{\boldsymbol{\omega}}_{11} = \boldsymbol{A}_1^\mathrm{T}\boldsymbol{M}_3+\boldsymbol{M}_3\boldsymbol{A}_1+\boldsymbol{L}_1\boldsymbol{M}_1\boldsymbol{L}_1+\mu\boldsymbol{I}$, $\tilde{\boldsymbol{\omega}}_{12} = \boldsymbol{A}_3^\mathrm{T}\bar{\boldsymbol{X}}_2+\boldsymbol{C}_1^\mathrm{T}\tilde{\boldsymbol{D}}_\mathrm{c}^\mathrm{T}+\boldsymbol{M}_3\boldsymbol{A}_2$, and $\tilde{\boldsymbol{\omega}}_{22} = \boldsymbol{A}_4^\mathrm{T}\bar{\boldsymbol{X}}_2+\boldsymbol{C}_2^\mathrm{T}\tilde{\boldsymbol{D}}_\mathrm{c}^\mathrm{T}+\bar{\boldsymbol{X}}_2\boldsymbol{A}_4+\tilde{\boldsymbol{D}}_\mathrm{c}\boldsymbol{C}_2+\boldsymbol{L}_2\boldsymbol{M}_2\boldsymbol{L}_2+\mu\boldsymbol{I}$. $\boldsymbol{M}_1$, $\boldsymbol{M}_2$, and $\boldsymbol{M}_3$ are positive definite matrices, and μ is a positive constant satisfying $\mu\ge 1+\gamma/\bar{\ell}$.

Consequently, set $\mathcal{A}$ is UGAS for the hybrid system $\mathcal{H}$.

Proof According to Definition 1, we can obtain that set $\mathcal{A}$ is UGAS if $\mathcal{A}$ is uniformly globally pre-asymptotically stable and the maximal solutions to $\mathcal{H}$ are complete. Clearly, because dom $\boldsymbol{z}$ is unbounded, the maximal solutions to $\mathcal{H}$ are complete. Hence, it remains to show that $\mathcal{A}$ is uniformly globally pre-asymptotically stable by adopting Lemma 1.

To begin with, assume that the system matrices in Eqs. (12) and (14) satisfy LMI (15). Let us consider the following Lyapunov function candidate:

$$\begin{aligned}V(\boldsymbol{z}) &= V_1(\boldsymbol{\zeta})+V_2(\boldsymbol{e},\tau)\\ &= \boldsymbol{\zeta}^\mathrm{T}\boldsymbol{P}\boldsymbol{\zeta}+U(\boldsymbol{e})\phi(\tau)\\ &= \boldsymbol{x}^\mathrm{T}\tilde{\boldsymbol{P}}_1\boldsymbol{x}+\boldsymbol{\xi}^\mathrm{T}\tilde{\boldsymbol{P}}_2\boldsymbol{\xi}+U(\boldsymbol{e})\phi(\tau),\end{aligned}$$

where $\tilde{\boldsymbol{P}}_1 = \operatorname{diag}(\boldsymbol{M}_3,\bar{\boldsymbol{X}}_2)$, $\tilde{\boldsymbol{P}}_2 = \bar{\boldsymbol{X}}_1$, $U(\boldsymbol{e}) = \kappa\boldsymbol{e}^\mathrm{T}\boldsymbol{e}$, and $\phi(\tau) = \bar{\phi}\boldsymbol{e}^{-\bar{\ell}\tau}$ with $\bar{\phi} = 1+\gamma/\bar{\ell}$. Hence, it follows that

$$V_1(\boldsymbol{\zeta}) \le V(\boldsymbol{z}) \le V_1(\boldsymbol{\zeta})+\bar{\phi}U(\boldsymbol{e}).$$

Define $\underline{\alpha}(\|\boldsymbol{z}\|_\mathcal{A}) = V_1(\boldsymbol{\zeta})$ and $V_1(\boldsymbol{\zeta})+\bar{\phi}U(\boldsymbol{e}) = \overline{\alpha}(\|\boldsymbol{z}\|_\mathcal{A})$. Clearly, functions $\underline{\alpha}$ and $\overline{\alpha}$ belong to class $\mathcal{K}_\infty$, which implies that inequality (9) in Lemma 1 holds. Next, considering the definitions of $V(\boldsymbol{\zeta})$, $\phi(\tau)$, $U(\boldsymbol{e})$, and the jump map $G(\boldsymbol{z})$ in Eq. (12), it follows that

$$V(g)-V(\boldsymbol{z}) = -U(\boldsymbol{e})\phi(\tau) \le 0, \tag{16}$$

which proves condition (10).

Later, to complete the proof of this theorem, we will show that condition (11) is satisfied; that is, for any given $\boldsymbol{z}\in\mathcal{F}$, there exists a positive definite function $\rho(\|\boldsymbol{z}\|_\mathcal{A})$ such that

$$\begin{aligned}&\langle\nabla V(\boldsymbol{z}),F(\boldsymbol{z})\rangle\\ =&\langle\nabla V_1(\boldsymbol{\zeta}),\dot{\boldsymbol{\zeta}}\rangle+\phi(\tau)\langle\nabla U(\boldsymbol{e}),\dot{\boldsymbol{e}}\rangle+U(\boldsymbol{e})\langle\nabla\phi(\tau),\dot{\tau}\rangle\\ =&\langle\nabla V_1(\boldsymbol{\zeta}),\tilde{f}_a(\boldsymbol{\zeta},\boldsymbol{e})\rangle+\phi(\tau)\langle\nabla U(\boldsymbol{e}),\tilde{f}_b(\boldsymbol{\zeta},\boldsymbol{e})\rangle\\ &-U(\boldsymbol{e})\bar{\ell}\phi(\tau)\\ \le&-\rho(\|\boldsymbol{z}\|_\mathcal{A}).\end{aligned} \tag{17}$$

$$\begin{bmatrix} \tilde{\boldsymbol{\omega}}_{11} & \tilde{\boldsymbol{\omega}}_{12} & \boldsymbol{C}_1^{\mathrm{T}}\tilde{\boldsymbol{B}}_{\mathrm{c}}^{\mathrm{T}} & \mathbf{0} & M_3\boldsymbol{B}_1 & M_3\boldsymbol{B}_2 & M_3 & \mathbf{0} & \boldsymbol{C}_1^{\mathrm{T}} \\ * & \tilde{\boldsymbol{\omega}}_{22} & \tilde{\boldsymbol{C}}_{\mathrm{c}}+\boldsymbol{C}_2^{\mathrm{T}}\tilde{\boldsymbol{B}}_{\mathrm{c}}^{\mathrm{T}} & \mathbf{0} & \bar{\boldsymbol{X}}_2B_3 & \bar{\boldsymbol{X}}_2\boldsymbol{B}_4 & \mathbf{0} & \bar{\boldsymbol{X}}_2 & \boldsymbol{C}_2^{\mathrm{T}} \\ * & * & \tilde{\boldsymbol{A}}_{\mathrm{c}}^{\mathrm{T}}+\tilde{\boldsymbol{A}}_{\mathrm{c}}+\mu\boldsymbol{I} & \bar{\boldsymbol{X}}_1 & \mathbf{0} & \mathbf{0} & \mathbf{0} & \mathbf{0} & \mathbf{0} \\ * & * & * & -\boldsymbol{N}_3 & \mathbf{0} & \mathbf{0} & \mathbf{0} & \mathbf{0} & \mathbf{0} \\ * & * & * & * & -\boldsymbol{M}_1 & \mathbf{0} & \mathbf{0} & \mathbf{0} & \mathbf{0} \\ * & * & * & * & * & -\boldsymbol{M}_2 & \mathbf{0} & \mathbf{0} & \mathbf{0} \\ * & * & * & * & * & * & -\boldsymbol{N}_1 & \mathbf{0} & \mathbf{0} \\ * & * & * & * & * & * & * & -\boldsymbol{N}_2 & \mathbf{0} \\ * & * & * & * & * & * & * & * & -\bar{\boldsymbol{X}}_3 \end{bmatrix} < 0. \tag{15}$$

To do so, we first separately deal with the Lie derivatives $\langle \nabla V_1(\boldsymbol{\zeta}), \tilde{f}_a(\boldsymbol{\zeta}, \boldsymbol{e})\rangle$ and $\langle \nabla U(\boldsymbol{e}), \tilde{f}_b(\boldsymbol{\zeta}, \boldsymbol{e})\rangle$. Substituting $\tilde{f}_a(\boldsymbol{\zeta}, \boldsymbol{e})$ into $\langle \nabla V_1(\boldsymbol{\zeta}), \tilde{f}_a(\boldsymbol{\zeta}, \boldsymbol{e})\rangle$ yields

$$\begin{aligned} &\langle \nabla V_1(\boldsymbol{\zeta}), \tilde{f}_a(\boldsymbol{\zeta}, \boldsymbol{e})\rangle \\ =&\dot{\boldsymbol{x}}^{\mathrm{T}}\tilde{\boldsymbol{P}}_1\boldsymbol{x}+\boldsymbol{x}^{\mathrm{T}}\tilde{\boldsymbol{P}}_1\dot{\boldsymbol{x}}+\dot{\boldsymbol{\xi}}^{\mathrm{T}}\tilde{\boldsymbol{P}}_2\boldsymbol{\xi}+\boldsymbol{\xi}^{\mathrm{T}}\tilde{\boldsymbol{P}}_2\dot{\boldsymbol{\xi}} \\ =&\boldsymbol{x}^{\mathrm{T}}\Big[(\boldsymbol{A}+\boldsymbol{E}\tilde{\boldsymbol{X}}_2\tilde{\boldsymbol{D}}_{\mathrm{c}}\boldsymbol{C})^{\mathrm{T}}\tilde{\boldsymbol{P}}_1 \\ &+\tilde{\boldsymbol{P}}_1(\boldsymbol{A}+\boldsymbol{E}\tilde{\boldsymbol{X}}_2\tilde{\boldsymbol{D}}_{\mathrm{c}}\boldsymbol{C})\Big]\boldsymbol{x} \\ &+\boldsymbol{\xi}^{\mathrm{T}}(\tilde{\boldsymbol{A}}_{\mathrm{c}}^{\mathrm{T}}\tilde{\boldsymbol{X}}_1\tilde{\boldsymbol{P}}_2+\boldsymbol{P}_2\tilde{\boldsymbol{X}}_1\tilde{\boldsymbol{A}}_{\mathrm{c}})\boldsymbol{\xi} \\ &+2f^{\mathrm{T}}(\boldsymbol{x})\boldsymbol{B}^{\mathrm{T}}\tilde{\boldsymbol{P}}_1\boldsymbol{x}+2\boldsymbol{e}^{\mathrm{T}}\tilde{\boldsymbol{D}}_{\mathrm{c}}^{\mathrm{T}}\tilde{\boldsymbol{X}}_2\boldsymbol{E}^{\mathrm{T}}\tilde{\boldsymbol{P}}_1\boldsymbol{x} \\ &+2\boldsymbol{e}^{\mathrm{T}}\tilde{\boldsymbol{B}}_{\mathrm{c}}^{\mathrm{T}}\tilde{\boldsymbol{X}}_1\tilde{\boldsymbol{P}}_2\boldsymbol{\xi}+2\boldsymbol{x}^{\mathrm{T}}\boldsymbol{C}^{\mathrm{T}}\tilde{\boldsymbol{B}}_{\mathrm{c}}^{\mathrm{T}}\tilde{\boldsymbol{X}}_1\tilde{\boldsymbol{P}}_2\boldsymbol{\xi} \\ &+2\boldsymbol{\xi}^{\mathrm{T}}\tilde{\boldsymbol{C}}_{\mathrm{c}}^{\mathrm{T}}\tilde{\boldsymbol{X}}_2\boldsymbol{E}^{\mathrm{T}}\tilde{\boldsymbol{P}}_1\boldsymbol{x}. \end{aligned} \tag{18}$$

Let $\tilde{\boldsymbol{Q}}_1 = \operatorname{diag}(\boldsymbol{M}_1, \boldsymbol{M}_2)$. According to Lemma 2 and the fact that f satisfies the Lipschitz condition (2), one has

$$\begin{aligned} &2f^{\mathrm{T}}(\boldsymbol{x})\boldsymbol{B}^{\mathrm{T}}\tilde{\boldsymbol{P}}_1\boldsymbol{x} \\ \le&\boldsymbol{x}^{\mathrm{T}}\tilde{\boldsymbol{P}}_1\boldsymbol{B}\tilde{\boldsymbol{Q}}_1^{-1}\boldsymbol{B}^{\mathrm{T}}\tilde{\boldsymbol{P}}_1\boldsymbol{x}+f^{\mathrm{T}}(\boldsymbol{x})\tilde{\boldsymbol{Q}}_1f(\boldsymbol{x}) \\ \le&\boldsymbol{x}^{\mathrm{T}}\left(\tilde{\boldsymbol{P}}_1\boldsymbol{B}\tilde{\boldsymbol{Q}}_1^{-1}\boldsymbol{B}^{\mathrm{T}}\tilde{\boldsymbol{P}}_1+\boldsymbol{L}\tilde{\boldsymbol{Q}}_1\boldsymbol{L}\right)\boldsymbol{x}, \\ &2\boldsymbol{e}^{\mathrm{T}}\tilde{\boldsymbol{D}}_{\mathrm{c}}^{\mathrm{T}}\tilde{\boldsymbol{X}}_2\boldsymbol{E}^{\mathrm{T}}\tilde{\boldsymbol{P}}_1\boldsymbol{x} \\ \le&\boldsymbol{x}^{\mathrm{T}}\tilde{\boldsymbol{P}}_1\boldsymbol{\Pi}_4^{-1}\tilde{\boldsymbol{P}}_1\boldsymbol{x}+\boldsymbol{e}^{\mathrm{T}}\tilde{\boldsymbol{D}}_{\mathrm{c}}^{\mathrm{T}}\tilde{\boldsymbol{X}}_2\boldsymbol{E}^{\mathrm{T}}\boldsymbol{\Pi}_4\boldsymbol{E}\tilde{\boldsymbol{X}}_2\tilde{\boldsymbol{D}}_{\mathrm{c}}\boldsymbol{e}, \\ &2\boldsymbol{e}^{\mathrm{T}}\tilde{\boldsymbol{B}}_{\mathrm{c}}^{\mathrm{T}}\tilde{\boldsymbol{X}}_1\boldsymbol{P}_2\boldsymbol{\xi} \\ \le&\boldsymbol{\xi}^{\mathrm{T}}\tilde{\boldsymbol{P}}_2\boldsymbol{N}_3^{-1}\tilde{\boldsymbol{P}}_2\boldsymbol{\xi}+\boldsymbol{e}^{\mathrm{T}}\tilde{\boldsymbol{B}}_{\mathrm{c}}^{\mathrm{T}}\tilde{\boldsymbol{X}}_1\boldsymbol{N}_3\tilde{\boldsymbol{X}}_1\tilde{\boldsymbol{B}}_{\mathrm{c}}\boldsymbol{e}, \end{aligned} \tag{19}$$

where $\boldsymbol{\Pi}_4$ and $\boldsymbol{N}_3$ are the positive definite matrices given in Eq. (13). Substituting inequality (19) into Eq. (18), we find that

$$\begin{aligned} &\langle \nabla V_1(\boldsymbol{\zeta}), \tilde{f}_a(\boldsymbol{\zeta}, \boldsymbol{e})\rangle \\ \le&\ \boldsymbol{\zeta}^{\mathrm{T}}\boldsymbol{\Lambda}_1\boldsymbol{\zeta}+\boldsymbol{e}^{\mathrm{T}}\boldsymbol{\Lambda}_2\boldsymbol{e}-\mu H(\boldsymbol{\zeta})-\delta(\boldsymbol{y}) \\ \le&\ \lambda_{\max}(\boldsymbol{\Lambda}_1)\boldsymbol{\zeta}^{\mathrm{T}}\boldsymbol{\zeta}+\lambda_{\max}(\boldsymbol{\Lambda}_2)\boldsymbol{e}^{\mathrm{T}}\boldsymbol{e}-\mu H(\boldsymbol{\zeta})-\delta(\boldsymbol{y}), \end{aligned} \tag{20}$$

where

$$\begin{aligned} &H(\boldsymbol{\zeta})=\boldsymbol{\zeta}^{\mathrm{T}}\boldsymbol{\zeta}, \\ &\boldsymbol{\Lambda}_1=\begin{bmatrix} \tilde{\boldsymbol{\omega}}_1 & \tilde{\boldsymbol{P}}_1^{\mathrm{T}}\boldsymbol{E}\tilde{\boldsymbol{X}}_2^{-1}\tilde{\boldsymbol{C}}_{\mathrm{c}}+\boldsymbol{C}^{\mathrm{T}}\tilde{\boldsymbol{B}}_{\mathrm{c}}^{\mathrm{T}}\tilde{\boldsymbol{X}}_1\tilde{\boldsymbol{P}}_2 \\ * & \tilde{\boldsymbol{A}}_{\mathrm{c}}^{\mathrm{T}}\tilde{\boldsymbol{X}}_1\tilde{\boldsymbol{P}}_2+\tilde{\boldsymbol{P}}_2\tilde{\boldsymbol{X}}_1\tilde{\boldsymbol{A}}_{\mathrm{c}}+\tilde{\boldsymbol{P}}_2^{\mathrm{T}}\tilde{\boldsymbol{Q}}_3^{-1}\tilde{\boldsymbol{P}}_2+\mu\boldsymbol{I} \end{bmatrix}, \\ &\boldsymbol{\Lambda}_2=\tilde{\boldsymbol{D}}_{\mathrm{c}}^{\mathrm{T}}\tilde{\boldsymbol{X}}_2\boldsymbol{E}^{\mathrm{T}}\boldsymbol{\Pi}_4\boldsymbol{E}\tilde{\boldsymbol{X}}_2\tilde{\boldsymbol{D}}_{\mathrm{c}}+\tilde{\boldsymbol{B}}_{\mathrm{c}}^{\mathrm{T}}\tilde{\boldsymbol{X}}_1\boldsymbol{N}_3\tilde{\boldsymbol{X}}_1\tilde{\boldsymbol{B}}_{\mathrm{c}}=\boldsymbol{\Xi}_2, \end{aligned}$$

in which

$$\begin{aligned} \tilde{\boldsymbol{\omega}}_1=&(\boldsymbol{A}+\boldsymbol{E}\tilde{\boldsymbol{X}}_2\tilde{\boldsymbol{D}}_{\mathrm{c}}\boldsymbol{C})^{\mathrm{T}}\tilde{\boldsymbol{P}}_1+\tilde{\boldsymbol{P}}_1(\boldsymbol{A}+\boldsymbol{E}\tilde{\boldsymbol{X}}_2\tilde{\boldsymbol{D}}_{\mathrm{c}}\boldsymbol{C}) \\ &+\boldsymbol{L}\tilde{\boldsymbol{Q}}_1\boldsymbol{L}+\tilde{\boldsymbol{P}}_1^{\mathrm{T}}\boldsymbol{B}\tilde{\boldsymbol{Q}}_1^{-1}\boldsymbol{B}^{\mathrm{T}}\tilde{\boldsymbol{P}}_1 \\ &+\tilde{\boldsymbol{P}}_1\boldsymbol{\Pi}_4^{-1}\tilde{\boldsymbol{P}}_1+\mu\boldsymbol{I}+\boldsymbol{C}^{\mathrm{T}}\tilde{\boldsymbol{X}}_3\boldsymbol{C}. \end{aligned}$$

Next, we deal with the following Lie derivative:

$$\begin{aligned} &\langle \nabla U(\boldsymbol{e}), \tilde{f}_b(\boldsymbol{\zeta}, \boldsymbol{e})\rangle=\kappa(\dot{\boldsymbol{e}}^{\mathrm{T}}\boldsymbol{e}+\boldsymbol{e}^{\mathrm{T}}\dot{\boldsymbol{e}}) \\ =&\kappa\boldsymbol{e}^{\mathrm{T}}(-\tilde{\boldsymbol{D}}_{\mathrm{c}}^{\mathrm{T}}\tilde{\boldsymbol{X}}_2\boldsymbol{E}^{\mathrm{T}}\boldsymbol{C}^{\mathrm{T}}-\boldsymbol{C}\boldsymbol{E}\tilde{\boldsymbol{X}}_2\tilde{\boldsymbol{D}}_{\mathrm{c}})\boldsymbol{e} \\ &-2\kappa\boldsymbol{\xi}^{\mathrm{T}}\tilde{\boldsymbol{C}}_{\mathrm{c}}^{\mathrm{T}}\tilde{\boldsymbol{X}}_2\boldsymbol{E}^{\mathrm{T}}\boldsymbol{C}^{\mathrm{T}}\boldsymbol{e}-2\kappa f^{\mathrm{T}}(\boldsymbol{x})\boldsymbol{B}^{\mathrm{T}}\boldsymbol{C}^{\mathrm{T}}\boldsymbol{e} \\ &-2\kappa\boldsymbol{x}^{\mathrm{T}}(\boldsymbol{A}+\boldsymbol{E}\tilde{\boldsymbol{X}}_2\tilde{\boldsymbol{D}}_{\mathrm{c}}\boldsymbol{C})^{\mathrm{T}}\boldsymbol{C}^{\mathrm{T}}\boldsymbol{e}. \end{aligned} \tag{21}$$

Similarly, using Lemma 2 and inequality (2), we obtain

$$\begin{aligned} &-2\boldsymbol{\xi}^{\mathrm{T}}\tilde{\boldsymbol{C}}_{\mathrm{c}}^{\mathrm{T}}\boldsymbol{X}_2\boldsymbol{E}^{\mathrm{T}}\boldsymbol{C}^{\mathrm{T}}\boldsymbol{e} \\ \le&\boldsymbol{\xi}^{\mathrm{T}}\tilde{\boldsymbol{C}}_{\mathrm{c}}^{\mathrm{T}}\boldsymbol{X}_2\boldsymbol{E}^{\mathrm{T}}\boldsymbol{C}^{\mathrm{T}}\boldsymbol{\Pi}_3\boldsymbol{C}\boldsymbol{E}\tilde{\boldsymbol{X}}_2\tilde{\boldsymbol{C}}_{\mathrm{c}}\boldsymbol{\xi}+\boldsymbol{e}^{\mathrm{T}}\boldsymbol{\Pi}_3^{-1}\boldsymbol{e}, \\ &-2\boldsymbol{x}^{\mathrm{T}}(\boldsymbol{A}+\boldsymbol{E}\tilde{\boldsymbol{X}}_2\tilde{\boldsymbol{D}}_{\mathrm{c}}\boldsymbol{C})^{\mathrm{T}}\boldsymbol{C}^{\mathrm{T}}\boldsymbol{e} \\ \le&\boldsymbol{x}^{\mathrm{T}}(\boldsymbol{A}+\boldsymbol{E}\tilde{\boldsymbol{X}}_2\tilde{\boldsymbol{D}}_{\mathrm{c}}\boldsymbol{C})^{\mathrm{T}}\boldsymbol{C}^{\mathrm{T}}\boldsymbol{\Pi}_2\boldsymbol{C}(\boldsymbol{A} \\ &+\boldsymbol{E}\tilde{\boldsymbol{X}}_2\tilde{\boldsymbol{D}}_{\mathrm{c}}\boldsymbol{C})\boldsymbol{x}+\boldsymbol{e}^{\mathrm{T}}\boldsymbol{\Pi}_2^{-1}\boldsymbol{e}, \\ &-2f^{\mathrm{T}}(\boldsymbol{x})\boldsymbol{B}^{\mathrm{T}}\boldsymbol{C}^{\mathrm{T}}\boldsymbol{e} \\ \le&f^{\mathrm{T}}(\boldsymbol{x})\boldsymbol{B}^{\mathrm{T}}\boldsymbol{C}^{\mathrm{T}}\boldsymbol{\Pi}_1\boldsymbol{C}\boldsymbol{B}f(\boldsymbol{x})+\boldsymbol{e}^{\mathrm{T}}\boldsymbol{\Pi}_1^{-1}\boldsymbol{e} \\ \le&\boldsymbol{x}^{\mathrm{T}}\boldsymbol{L}\boldsymbol{B}^{\mathrm{T}}\boldsymbol{C}^{\mathrm{T}}\boldsymbol{\Pi}_1\boldsymbol{C}\boldsymbol{B}\boldsymbol{L}\boldsymbol{x}+\boldsymbol{e}^{\mathrm{T}}\boldsymbol{\Pi}_1^{-1}\boldsymbol{e}, \end{aligned} \tag{22}$$

where $\boldsymbol{\Pi}_1$, $\boldsymbol{\Pi}_2$, and $\boldsymbol{\Pi}_3$ are the positive definite matrices given in Eq. (13). Consequently, we obtain

$$\begin{aligned} &\langle \nabla U(\boldsymbol{e}), \tilde{f}_b(\boldsymbol{\zeta}, \boldsymbol{e})\rangle \\ \le&\kappa\boldsymbol{\zeta}^{\mathrm{T}}\boldsymbol{\Xi}_1\boldsymbol{\zeta}+\kappa\boldsymbol{e}^{\mathrm{T}}\boldsymbol{\Xi}_3\boldsymbol{e} \\ \le&\kappa\lambda_{\max}(\boldsymbol{\Xi}_1)\boldsymbol{\zeta}^{\mathrm{T}}\boldsymbol{\zeta}+\kappa\lambda_{\max}(\boldsymbol{\Xi}_3)\boldsymbol{e}^{\mathrm{T}}\boldsymbol{e} \\ \le&H(\boldsymbol{\zeta})+\ell U(\boldsymbol{e}). \end{aligned} \tag{23}$$

Combining inequalities (17), (20), and (23) leads to

$$\begin{aligned}&\langle\nabla V(\boldsymbol{z}), F(\boldsymbol{z})\rangle\\ \leq&\lambda_{\max}(\boldsymbol{\Lambda}_1)\boldsymbol{\zeta}^{\mathrm{T}}\boldsymbol{\zeta}+\lambda_{\max}(\boldsymbol{\Xi}_2)\boldsymbol{e}^{\mathrm{T}}\boldsymbol{e}-\mu H(\boldsymbol{\zeta})\\ &-\delta(\boldsymbol{y})+\phi(H(\boldsymbol{\zeta})+\ell U(\boldsymbol{e}))-\bar{\ell}U(\boldsymbol{e})\phi(\tau)\\ =&-\alpha(\|\boldsymbol{\zeta}\|)+\gamma U(\boldsymbol{e})-(\mu-\phi)H(\boldsymbol{\zeta})-\delta(\boldsymbol{y})\\ &-(\bar{\ell}-\ell)\phi U(\boldsymbol{e}),\end{aligned}\tag{24}$$

where $\alpha\left(\|\boldsymbol{\zeta}\|\right)=-\lambda_{\max}(\boldsymbol{\Lambda}_1)\boldsymbol{\zeta}^{\mathrm{T}}\boldsymbol{\zeta}$.

Let $\rho_1(\|\boldsymbol{z}\|_{\mathcal{A}})=\alpha(\|\boldsymbol{\zeta}\|)$, $\rho_2(\|\boldsymbol{z}\|_{\mathcal{A}})=(\mu-\phi)H(\boldsymbol{\zeta})$, and $\rho_3(\|\boldsymbol{z}\|_{\mathcal{A}})=\delta(\boldsymbol{y})-\gamma U(\boldsymbol{e})+(\bar{\ell}-\ell)\phi U(\boldsymbol{e})$. We will prove that ρ_1, ρ_2, and ρ_3 belong to class $\mathcal{PD}$.

To prove that ρ_1 belongs to class $\mathcal{PD}$, we need to prove that $\boldsymbol{\Lambda}_1<0$. By Lemma 3 and the fact that $\mathrm{diag}(\tilde{\boldsymbol{Q}}_3,\tilde{\boldsymbol{Q}}_1,\boldsymbol{\Pi}_4,\bar{\boldsymbol{X}}_3)>0$, we have $\boldsymbol{\Lambda}_1<0$ if the following matrix inequality

$$\begin{bmatrix}\tilde{\boldsymbol{\omega}}_{11} & \tilde{\boldsymbol{\omega}}_{12} & \boldsymbol{0} & \tilde{\boldsymbol{P}}_1\boldsymbol{B} & \tilde{\boldsymbol{P}}_1 & \boldsymbol{C}^{\mathrm{T}}\\ * & \tilde{\boldsymbol{\omega}}_{22} & \tilde{\boldsymbol{P}}_2 & \boldsymbol{0} & \boldsymbol{0} & \boldsymbol{0}\\ * & * & -\tilde{\boldsymbol{Q}}_3 & \boldsymbol{0} & \boldsymbol{0} & \boldsymbol{0}\\ * & * & * & -\tilde{\boldsymbol{Q}}_1 & \boldsymbol{0} & \boldsymbol{0}\\ * & * & * & * & -\boldsymbol{\Pi}_4 & \boldsymbol{0}\\ * & * & * & * & * & -\bar{\boldsymbol{X}}_3\end{bmatrix}<0\tag{25}$$

holds, in which $\tilde{\boldsymbol{\omega}}_{11}=(\boldsymbol{A}+\boldsymbol{E}\tilde{\boldsymbol{X}}_2\tilde{\boldsymbol{D}}_{\mathrm{c}}\boldsymbol{C})^{\mathrm{T}}\tilde{\boldsymbol{P}}_1+\tilde{\boldsymbol{P}}_1(\boldsymbol{A}+\boldsymbol{E}\tilde{\boldsymbol{X}}_2\tilde{\boldsymbol{D}}_{\mathrm{c}}\boldsymbol{C})+\boldsymbol{L}\tilde{\boldsymbol{Q}}_1\boldsymbol{L}+\mu\boldsymbol{I}$, $\tilde{\boldsymbol{\omega}}_{12}=\tilde{\boldsymbol{P}}_1^{\mathrm{T}}\boldsymbol{E}\tilde{\boldsymbol{X}}_2^{-1}\tilde{\boldsymbol{C}}_{\mathrm{c}}+\boldsymbol{C}^{\mathrm{T}}\tilde{\boldsymbol{B}}_{\mathrm{c}}^{\mathrm{T}}\tilde{\boldsymbol{X}}_1\tilde{\boldsymbol{P}}_2$, and $\tilde{\boldsymbol{\omega}}_{22}=\tilde{\boldsymbol{A}}_{\mathrm{c}}^{\mathrm{T}}\tilde{\boldsymbol{X}}_1\tilde{\boldsymbol{P}}_2+\tilde{\boldsymbol{P}}_2\tilde{\boldsymbol{X}}_1\tilde{\boldsymbol{A}}_{\mathrm{c}}+\mu\boldsymbol{I}$. Moreover, considering

$$\begin{aligned}&(\boldsymbol{A}+\boldsymbol{E}\tilde{\boldsymbol{X}}_2\tilde{\boldsymbol{D}}_{\mathrm{c}}\boldsymbol{C})^{\mathrm{T}}\tilde{\boldsymbol{P}}_1\\ =&\begin{bmatrix}\boldsymbol{A}_1^{\mathrm{T}} & (\boldsymbol{A}_3+\tilde{\boldsymbol{X}}_2\tilde{\boldsymbol{D}}_{\mathrm{c}}\boldsymbol{C}_1)^{\mathrm{T}}\\ \boldsymbol{A}_2^{\mathrm{T}} & (\boldsymbol{A}_4+\tilde{\boldsymbol{X}}_2\tilde{\boldsymbol{D}}_{\mathrm{c}}\boldsymbol{C}_2)^{\mathrm{T}}\end{bmatrix}\begin{bmatrix}\boldsymbol{M}_3 & \boldsymbol{0}\\ \boldsymbol{0} & \tilde{\boldsymbol{X}}_2^{-1}\end{bmatrix}\\ =&\begin{bmatrix}\boldsymbol{A}_1^{\mathrm{T}}\boldsymbol{M}_3 & \boldsymbol{A}_3^{\mathrm{T}}\tilde{\boldsymbol{X}}_2^{-1}+\boldsymbol{C}_1^{\mathrm{T}}\tilde{\boldsymbol{D}}_{\mathrm{c}}^{\mathrm{T}}\\ \boldsymbol{A}_2^{\mathrm{T}}\boldsymbol{M}_3 & \boldsymbol{A}_4\tilde{\boldsymbol{X}}_2^{-1}+\boldsymbol{C}_2^{\mathrm{T}}\tilde{\boldsymbol{D}}_{\mathrm{c}}^{\mathrm{T}}\end{bmatrix},\end{aligned}$$

$$\begin{aligned}&\tilde{\boldsymbol{P}}_1^{\mathrm{T}}\boldsymbol{E}\tilde{\boldsymbol{X}}_2\tilde{\boldsymbol{C}}_{\mathrm{c}}+\boldsymbol{C}^{\mathrm{T}}\tilde{\boldsymbol{B}}_{\mathrm{c}}^{\mathrm{T}}\tilde{\boldsymbol{X}}_1\tilde{\boldsymbol{P}}_2\\ =&\begin{bmatrix}\boldsymbol{M}_3 & \boldsymbol{0}\\ \boldsymbol{0} & \tilde{\boldsymbol{X}}_2^{-1}\end{bmatrix}\begin{bmatrix}\boldsymbol{0}\\ \boldsymbol{I}\end{bmatrix}\tilde{\boldsymbol{X}}_2\tilde{\boldsymbol{C}}_{\mathrm{c}}+\begin{bmatrix}\boldsymbol{C}_1^{\mathrm{T}}\\ \boldsymbol{C}_2^{\mathrm{T}}\end{bmatrix}\tilde{\boldsymbol{B}}_{\mathrm{c}}^{\mathrm{T}}\tilde{\boldsymbol{X}}_1\tilde{\boldsymbol{P}}_2\\ =&\begin{bmatrix}\boldsymbol{C}_1^{\mathrm{T}}\tilde{\boldsymbol{B}}_{\mathrm{c}}^{\mathrm{T}}\\ \tilde{\boldsymbol{C}}_{\mathrm{c}}+\boldsymbol{C}_2^{\mathrm{T}}\tilde{\boldsymbol{B}}_{\mathrm{c}}^{\mathrm{T}}\end{bmatrix},\end{aligned}$$

$$\begin{aligned}\boldsymbol{L}\tilde{\boldsymbol{Q}}_1\boldsymbol{L}&=\begin{bmatrix}\boldsymbol{L}_1 & \boldsymbol{0}\\ \boldsymbol{0} & \boldsymbol{L}_2\end{bmatrix}\begin{bmatrix}\boldsymbol{M}_1 & \boldsymbol{0}\\ \boldsymbol{0} & \boldsymbol{M}_2\end{bmatrix}\begin{bmatrix}\boldsymbol{L}_1 & \boldsymbol{0}\\ \boldsymbol{0} & \boldsymbol{L}_2\end{bmatrix}\\ &=\begin{bmatrix}\boldsymbol{L}_1\boldsymbol{M}_1\boldsymbol{L}_1 & \boldsymbol{0}\\ \boldsymbol{0} & \boldsymbol{L}_2^{\mathrm{T}}\boldsymbol{M}_2\boldsymbol{L}_2\end{bmatrix},\end{aligned}$$

$$\begin{aligned}\tilde{\boldsymbol{P}}_1\boldsymbol{B}&=\begin{bmatrix}\boldsymbol{M}_3 & \boldsymbol{0}\\ \boldsymbol{0} & \tilde{\boldsymbol{X}}_2^{-1}\end{bmatrix}\begin{bmatrix}\boldsymbol{B}_1 & \boldsymbol{B}_2\\ \boldsymbol{B}_3 & \boldsymbol{B}_4\end{bmatrix}\\ &=\begin{bmatrix}\boldsymbol{M}_3\boldsymbol{B}_1 & \boldsymbol{M}_3\boldsymbol{B}_2\\ \tilde{\boldsymbol{X}}_2^{-1}\boldsymbol{B}_3 & \tilde{\boldsymbol{X}}_2^{-1}\boldsymbol{B}_4\end{bmatrix},\end{aligned}$$

it follows that inequality (25) is equivalent to inequality (15). Therefore, inequality (15) implies that ρ_1 belongs to $\mathcal{PD}$.

Moreover, according to the definition of μ, it follows that $\mu\geq 1+\gamma/\bar{\ell}\geq\phi(\tau)$. This indicates that ρ_2 also belongs to $\mathcal{PD}$. Hence, it remains to show that ρ_3 also belongs to class $\mathcal{PD}$.

As for ρ_3, recalling the definition of the flow set $\mathcal{F}$, we distinguish the following two cases: (1) $\gamma U(\boldsymbol{e})-\delta(\boldsymbol{y})\leq 0$ and (2) $\gamma U(\boldsymbol{e})-\delta(\boldsymbol{y})>0$ while $\tau\in[0,\bar{\tau}]$.

Case 1: Suppose that $-\delta(\boldsymbol{y})+\gamma U(\boldsymbol{e})\leq 0$ is satisfied. It follows that

$$\rho_3(\|\boldsymbol{z}\|_{\mathcal{A}})\geq(\bar{\ell}-\ell)\phi U(\boldsymbol{e}),$$

which implies that $\rho_3\in\mathcal{PD}$, and thus inequality (17) is proved.

Case 2: Suppose that $\gamma U(\boldsymbol{e})-\delta(\boldsymbol{y})>0$ while $\tau\in[0,\bar{\tau}]$, which implies that

$$\gamma/(\bar{\ell}-\ell)=\phi(\bar{\tau})\leq\phi(\tau)\leq\phi(0)=\bar{\phi}\leq\mu.$$

It leads to $-\gamma U(\boldsymbol{e})+(\bar{\ell}-\ell)\phi U(\boldsymbol{e})\geq 0$. Recalling that $\delta(\boldsymbol{y})\geq 0$, we have $\rho_3\in\mathcal{PD}$, and thus condition (17) is satisfied.

Due to the nature of F, G, $\mathcal{F}$, and $\mathcal{J}$, scaling an initial condition by a positive constant causes solutions that are scaled by the same constant. Therefore, it follows that, except for solutions starting at the origin, each jump is followed by flowing for at least $\bar{\tau}$ units of time. In particular, $(t,j)\in\mathrm{dom}\ \boldsymbol{z}$ implies that $j\leq 1+t/\bar{\tau}$. In turn, $(t,j)\in\mathrm{dom}\ \boldsymbol{z}$ and $t+j\geq T$ imply $t\geq(T-1)\bar{\tau}/(\bar{\tau}+1)=T\bar{\tau}/(\bar{\tau}+1)-\bar{\tau}/(\bar{\tau}+1)$. Let $\gamma_r(T)=T\bar{\tau}/(\bar{\tau}+1)$ and $N_r=\bar{\tau}/(\bar{\tau}+1)$. Clearly, $\gamma_r\in\mathcal{K}_\infty$ and $N_r\geq 0$. This satisfies the additional condition in Lemma 1. In summary, we have proven that set $\mathcal{A}$ is UGAS for the hybrid system $\mathcal{H}$.

Remark 3 In Theorem 2, the Zeno phenomenon can be avoided due to the existence of the minimum inter-event interval $\bar{\tau}\in\left(0,\frac{1}{\bar{\ell}}\ln\left(\frac{\gamma-\ell+\bar{\ell}}{\gamma}+\frac{\ell}{\bar{\ell}}\right)\right]$. That is, the system will not jump into set $\mathcal{J}$ after the former jump occurs within $\bar{\tau}$ units of time. Moreover, it is noted that the parameters ℓ and γ can be chosen in different ways. For instance, if we take ℓ to be any positive value larger than $\max\{\lambda_{\max}(\boldsymbol{\Xi}_3),2\gamma\}$, then the upper bound of the minimum inter-event interval $\bar{\tau}$ will decrease. Similarly, if we take a smaller γ, the upper bound of $\bar{\tau}$ will get smaller.

Remark 4 It is worth pointing out that in Theorem 2, the controller gains are determined by the positive definite matrices $\boldsymbol{N}_1$, $\boldsymbol{N}_2$, $\boldsymbol{N}_3$, $\boldsymbol{M}_1$, $\boldsymbol{M}_2$, $\boldsymbol{\Pi}_1$, $\boldsymbol{\Pi}_2$, $\boldsymbol{\Pi}_3$, $\tilde{\boldsymbol{X}}_4$ and LMI (15). In practice, to simplify the computation, one can choose $\boldsymbol{M}_1 = q_1\boldsymbol{I}$, $\boldsymbol{M}_2 = q_2\boldsymbol{I}$, $\boldsymbol{N}_1 = q_3\boldsymbol{I}$, $\boldsymbol{N}_2 = q_4\boldsymbol{I}$, $\boldsymbol{N}_3 = q_5\boldsymbol{I}$, $\boldsymbol{\Pi}_1 = q_6\boldsymbol{I}$, $\boldsymbol{\Pi}_2 = q_7\boldsymbol{I}$, $\boldsymbol{\Pi}_3 = q_8\boldsymbol{I}$, and $\bar{\boldsymbol{X}}_3 = q_9\boldsymbol{I}$, where $q_i > 0$ $(i = 1, 2, \ldots, 9)$. Consequently, we can achieve the desired control effect by adjusting the selection of q_i $(i = 1, 2, \ldots, 9)$.

Remark 5 Note that the LMI condition in Theorem 1 is less conservative than that in Theorem 2. According to the LMI condition in Theorem 2, the feasible solutions of $\boldsymbol{A}_\mathrm{c}$, $\boldsymbol{B}_\mathrm{c}$, $\boldsymbol{C}_\mathrm{c}$, and $\boldsymbol{D}_\mathrm{c}$ are included in the feasible solutions of Theorem 1. If no feasible solutions of LMI in Theorem 2 exist, we can use Theorem 1, but bear a higher control burden.

4 Numerical simulations

In this section, we will present two numerical examples to illustrate the effectiveness and applicability of our proposed methodologies. More explicitly, we first introduce an unstable neural network system and show that both the proposed continuous-time and event-triggered dynamic output-feedback controllers are able to stabilize this network system. Later, we adopt a genetic regulatory network system, which is also unstable, to illustrate the difference between event-triggered dynamic output-feedback controllers and static controllers.

Example 1 Consider a neural network of the following form (Sanchez and Perez, 2003):

$$\dot{\boldsymbol{x}} = \boldsymbol{A}\boldsymbol{x} + \boldsymbol{B}f(\boldsymbol{x}),$$

where $\boldsymbol{A} = \begin{bmatrix} -2 & 0 \\ 0 & -2 \end{bmatrix}$, $\boldsymbol{B} = \begin{bmatrix} 1 & 2 \\ -3 & 4 \end{bmatrix}$, and $f(\boldsymbol{x}) = \begin{bmatrix} \tanh(x_1) \\ \tanh(x_2) \end{bmatrix}$. By taking $y = x_2$ as the output and imposing the input into the dynamics of x_2, the above network system can be rewritten as

$$\begin{aligned} \dot{\boldsymbol{x}} &= \boldsymbol{A}\boldsymbol{x} + \boldsymbol{B}f(\boldsymbol{x}) + \boldsymbol{E}u, \\ y &= \boldsymbol{C}\boldsymbol{x}, \end{aligned} \tag{26}$$

where $\boldsymbol{E} = [0 \quad 1]^\mathrm{T}$ and $\boldsymbol{C} = [0 \quad 1]$. Clearly, function $f(\boldsymbol{x})$ satisfies the Lipschitz conditions; i.e., it holds that

$$f^\mathrm{T}(\boldsymbol{x})\boldsymbol{Q}f(\boldsymbol{x}) \le \boldsymbol{x}^\mathrm{T}\boldsymbol{Q}\boldsymbol{x},$$

where $\boldsymbol{Q}$ is any positive definite matrix. This implies that system (26) has an equilibrium $\boldsymbol{x} = [0, 0]^\mathrm{T}$ when the input is absent. One can verify that this equilibrium is unstable for system (26). Take the initial states as

$$[x_1(0), x_2(0)]^\mathrm{T} = [3, 4]^\mathrm{T}.$$

The evolution trajectory of states x_1 and x_2 are depicted in Fig. 2a.

Recall the proposed event-triggered dynamic output-feedback controller design method and construct the following event-triggered output-feedback controller:

$$\begin{aligned} \dot{\xi} &= A_\mathrm{c}\xi + B_\mathrm{c}\bar{y}, \\ u &= C_\mathrm{c}\xi + D_\mathrm{c}\bar{y}, \end{aligned} \tag{27}$$

where $\bar{y} = y(t_k)$ with t_k being the k^th event-triggered time, and A_c, B_c, C_c, and D_c are scalers here, which will be determined later. Combining Eqs. (26) and (27), we have the following hybrid system:

$$\mathcal{H}: \begin{cases} \begin{cases} \dot{\boldsymbol{\zeta}} = f_1(\boldsymbol{\zeta}, e) \\ \dot{e} = f_2(\boldsymbol{\zeta}, e) \\ \dot{\tau} = 1 \end{cases} & (\boldsymbol{\zeta}, e, \tau) \in \mathcal{F}, \\ \begin{cases} \boldsymbol{\zeta}^+ = \boldsymbol{\zeta} \\ e^+ = 0 \\ \tau^+ = 0 \end{cases} & (\boldsymbol{\zeta}, e, \tau) \in \mathcal{J}, \end{cases} \tag{28}$$

where $\boldsymbol{\zeta} := \mathrm{col}(\boldsymbol{x}, \xi)$, $\tau \ge 0$ is the timer variable, $e := \bar{y} - y$, and

$$\begin{aligned} f_1(\boldsymbol{\zeta}, e) = &\begin{bmatrix} \boldsymbol{A} + \boldsymbol{E}D_\mathrm{c}\boldsymbol{C} & \boldsymbol{E}C_\mathrm{c} \\ B_\mathrm{c}\boldsymbol{C} & A_\mathrm{c} \end{bmatrix}\boldsymbol{\zeta} \\ &+ \begin{bmatrix} \boldsymbol{B}f(\boldsymbol{x}) \\ 0 \end{bmatrix} + \begin{bmatrix} \boldsymbol{E}D_\mathrm{c} \\ B_\mathrm{c} \end{bmatrix} e, \\ f_2(\boldsymbol{\zeta}, e) = &-\boldsymbol{C}\Big([\boldsymbol{A} + \boldsymbol{E}D_\mathrm{c}\boldsymbol{C} \quad \boldsymbol{E}C_\mathrm{c}]\boldsymbol{\zeta} \\ &+ \boldsymbol{B}f(\boldsymbol{x}) + \boldsymbol{E}D_\mathrm{c}e\Big). \end{aligned}$$

According to Remark 4, taking $q_1 = 50$, $q_2 = 100$, $q_3 = 100$, $q_4 = 0.5$, $q_5 = 5$, $q_6 = 0.1$, $q_7 = 0.002$, $q_8 = 0.001$, and $q_9 = 0.8$, and using the MATLAB LMI toolbox to compute inequality (15), the gains in controller (27) are calculated as follows: $A_\mathrm{c} = -2.5444$, $B_\mathrm{c} = 3.9370$, $C_\mathrm{c} = -15.6423$, and $D_\mathrm{c} = -18.0449$. Moreover, by Theorem 2, it yields $\gamma = 737.2263$, $\ell = 1546.0898$. Then, we can obtain the upper bound of the minimum inter-event interval $\bar{\tau}$ as 0.4483 ms. In the simulations, we choose $\bar{\tau} = 0.4483$ ms. Then, sets $\mathcal{F}$ and $\mathcal{J}$ will be determined by

$$\mathcal{F} = \{(\boldsymbol{\zeta}, e, \tau) : 240.3072 e^{\mathrm{T}} e \leq y^{\mathrm{T}} y \text{ or } \tau \in [0, 0.000\,448\,3]\},$$
$$\mathcal{J} = \{(\boldsymbol{\zeta}, e, \tau) : 240.3072 e^{\mathrm{T}} e \geq y^{\mathrm{T}} y \text{ and } \tau \geq 0.000\,448\,3\}.$$

Take the initial states as $[x_1(0), x_2(0)]^{\mathrm{T}} = [3, 4]^{\mathrm{T}}$, $[\xi(0), e(0), \tau(0)]^{\mathrm{T}} = [0, 0, 0]^{\mathrm{T}}$. It can be seen from Fig. 2b that the states x_1 and x_2 converge to zero gradually under event-triggered dynamic output-feedback control, which means that the closed-loop hybrid system (28) is globally asymptotically stable. Define the event intervals as $\delta_k = t_{k+1} - t_k$ with $k = 0, 1, \ldots$ (Fig. 2c). The figure reflects the relationships between the triggering instants and the triggering intervals. It turns out that the sequence of $\{\delta_k\}$ is a combination of two kinds of intervals: one is larger than $\bar{\tau}$ and the other is equal to $\bar{\tau}$. Intuitively, the former is caused by the condition $240.3072 e^{\mathrm{T}} e \geq y^{\mathrm{T}} y$, and the latter one is a result of the minimum event-triggered interval constraint, which also prevents the Zeno phenomenon of system (28).

In addition, to compare the effectiveness of continuous-time and event-triggered control, consider the following continuous-time dynamic output-feedback controller:

$$\begin{aligned} \dot{\xi} &= A_{\mathrm{c}} \xi + B_{\mathrm{c}} y, \\ u &= C_{\mathrm{c}} \xi + D_{\mathrm{c}} y. \end{aligned} \tag{29}$$

Because the designed controller gains in the continuous-time dynamic output-feedback controller also satisfy condition (5) in Theorem 1, we have that the obtained continuous-time closed-loop system is globally asymptotically stable (Fig. 2d). Note that the controller gains in Eq. (29) are the same as those

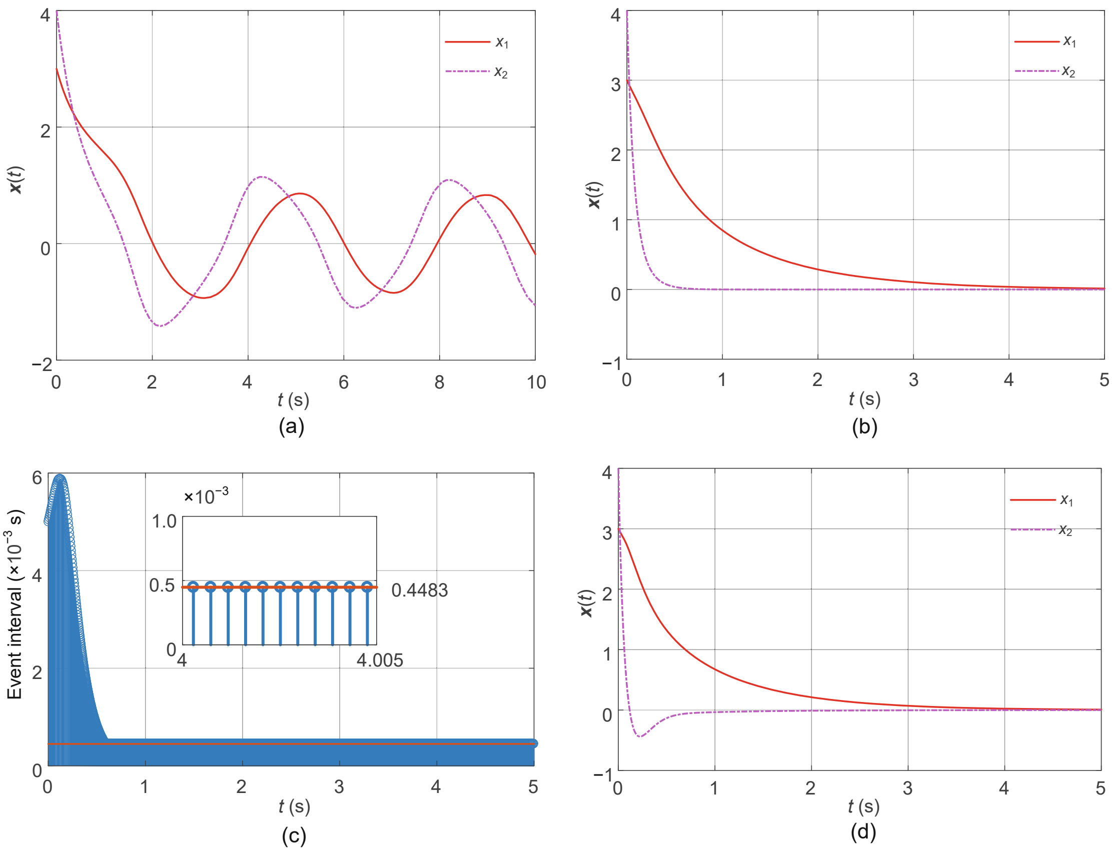

Fig. 2 Simulation results of Example 1: (a) evolutions of $x(t)$ of the original system; (b) evolutions of $x(t)$ of the closed-loop system under event-triggered dynamic output-feedback control; (c) evolutions of the intervals of event-triggered instants (the height of each vertical line shows the triggering interval between the current triggering instant and the last triggering instant); (d) evolutions of $x(t)$ of the closed-loop system under continuous-time dynamic output-feedback control

in the event-triggered dynamic output-feedback controller. This situation reflects the fact that these two closed-loop systems have similar convergence time. However, the event-triggered control method reduces the number of transmission times and the control burden.

Example 2 Consider a genetic regulatory network system of the following form (Li and Sun, 2010):

$$\dot{\boldsymbol{p}} = \boldsymbol{A}\boldsymbol{p} + \boldsymbol{B}f(\boldsymbol{p}), \tag{30}$$

where $\boldsymbol{p} = [p_1, p_2]^{\mathrm{T}}$, $\boldsymbol{A} = \begin{bmatrix} -5 & 5 \\ 5 & -5 \end{bmatrix}$, $\boldsymbol{B} = \begin{bmatrix} -1 & -1 \\ -2 & 0 \end{bmatrix}$, and $f(\boldsymbol{p}) = \begin{bmatrix} 1/(1+p_1^2) \\ 1/(1+p_2^2) \end{bmatrix}$. Because $1/(1+p^2) = 1-p^2/(1+p^2)$, Eq. (30) can be rewritten as

$$\dot{\boldsymbol{p}} = \boldsymbol{A}\boldsymbol{p} - \boldsymbol{B}\bar{f}(\boldsymbol{p}) + \boldsymbol{v}, \tag{31}$$

where $\bar{f}(\boldsymbol{p}) = \begin{bmatrix} p_1^2/(1+p_1^2) \\ p_2^2/(1+p_2^2) \end{bmatrix}$ and $\boldsymbol{v} = \begin{bmatrix} -2 \\ -2 \end{bmatrix}$. It can be verified that state $\boldsymbol{p}^* = [61.1133, 61.1133]^{\mathrm{T}}$ is an unstable equilibrium of system (31). Taking the initial states as $\boldsymbol{p}(0) = [30, 80]^{\mathrm{T}}$, the evolution trajectories of states p_1 and p_2 are as shown in Fig. 3a. Let $\boldsymbol{x} = \boldsymbol{p} - \boldsymbol{p}^*$; hence, the error system is obtained as

$$\dot{\boldsymbol{x}} = \boldsymbol{A}\boldsymbol{x} + \bar{\boldsymbol{B}}g(\boldsymbol{x}), \tag{32}$$

where $\bar{\boldsymbol{B}} = -\boldsymbol{B}$, $g(\boldsymbol{x}) = \bar{f}(\boldsymbol{x}+\boldsymbol{p}^*) - \bar{f}(\boldsymbol{p}^*)$. Note that thanks to the form of $\bar{f}$, $g(\boldsymbol{x})$ satisfies the Lipchitz conditions and for any $\boldsymbol{Q} > 0$, $g^{\mathrm{T}}(\boldsymbol{x})\boldsymbol{Q}g(\boldsymbol{x}) \leq 0.25\boldsymbol{x}^{\mathrm{T}}\boldsymbol{Q}\boldsymbol{x}$ holds.

By taking $y = x_2$ as the output and considering the input u, the above error system can be rewritten as

$$\begin{aligned} \dot{\boldsymbol{x}} &= \boldsymbol{A}\boldsymbol{x} + \bar{\boldsymbol{B}}g(\boldsymbol{x}) + \boldsymbol{E}u, \\ y &= \boldsymbol{C}\boldsymbol{x}, \end{aligned} \tag{33}$$

where $\boldsymbol{E} = [0 \quad 1]^{\mathrm{T}}$, $\boldsymbol{C} = [0 \quad 1]$. Similarly, combining Eqs. (27) and (33), we have the following hybrid system:

$$\mathcal{H}: \begin{cases} \begin{cases} \dot{\boldsymbol{\zeta}} = f_1(\boldsymbol{\zeta}, e) \\ \dot{e} = f_2(\boldsymbol{\zeta}, e) & (\boldsymbol{\zeta}, e, \tau) \in \mathcal{F}, \\ \dot{\tau} = 1 \end{cases} \\ \begin{cases} \boldsymbol{\zeta}^+ = \boldsymbol{\zeta} \\ e^+ = 0 & (\boldsymbol{\zeta}, e, \tau) \in \mathcal{J}, \\ \tau^+ = 0 \end{cases} \end{cases} \tag{34}$$

where $\boldsymbol{\zeta} := \mathrm{col}(\boldsymbol{x}, \xi)$, $\tau \geq 0$ is the timer variable, $e := \bar{y} - y$,

$$\begin{aligned} f_1(\boldsymbol{\zeta}, e) =& \begin{bmatrix} \boldsymbol{A} + \boldsymbol{E}D_{\mathrm{c}}\boldsymbol{C} & \boldsymbol{E}C_{\mathrm{c}} \\ B_{\mathrm{c}}\boldsymbol{C} & A_{\mathrm{c}} \end{bmatrix} \boldsymbol{\zeta} \\ &+ \begin{bmatrix} \bar{\boldsymbol{B}}g(\boldsymbol{x}) \\ 0 \end{bmatrix} + \begin{bmatrix} \boldsymbol{E}D_{\mathrm{c}} \\ B_{\mathrm{c}} \end{bmatrix} e, \\ f_2(\boldsymbol{\zeta}, e) =& -\boldsymbol{C}\Big([\boldsymbol{A} + \boldsymbol{E}D_{\mathrm{c}}\boldsymbol{C} \quad \boldsymbol{E}C_{\mathrm{c}}]\boldsymbol{\zeta} \\ &+ \bar{\boldsymbol{B}}g(\boldsymbol{x}) + \boldsymbol{E}D_{\mathrm{c}}e\Big). \end{aligned}$$

According to Remark 4, taking $q_1 = 0.8$, $q_2 = 130$, $q_3 = 100$, $q_4 = 0.5$, $q_5 = 5$, $q_6 = 0.2$, $q_7 = 0.002$, $q_8 = 0.002$, and $q_9 = 1$, and using the MATLAB LMI toolbox to compute inequality (15), the gains in controller (27) are calculated as follows: $A_{\mathrm{c}} = -3.9406$, $B_{\mathrm{c}} = 5.4912$, $C_{\mathrm{c}} = -23.9696$, and $D_{\mathrm{c}} = -21.6673$. Moreover, by Theorem 2, it yields $\gamma = 570.5843$, $\ell = 1141.1686$. Then, we can obtain the upper bound of the minimum inter-event interval $\bar{\tau}$ as 0.61 ms. In the simulations, we choose $\bar{\tau} = 0.61$ ms. Then, sets $\mathcal{F}$ and $\mathcal{J}$ will be determined by

$$\begin{aligned} \mathcal{F} =& \big\{(\boldsymbol{\zeta}, e, \tau) : 959.8677e^{\mathrm{T}}e \leq y^{\mathrm{T}}y \\ & \text{or } \tau \in [0, 0.000\,61]\big\}, \\ \mathcal{J} =& \big\{(\boldsymbol{\zeta}, e, \tau) : 959.8677e^{\mathrm{T}}e \geq y^{\mathrm{T}}y \\ & \text{and } \tau \geq 0.000\,61\big\}. \end{aligned}$$

Take the initial states as $[x_1(0), x_2(0)]^{\mathrm{T}} = [30, 80]^{\mathrm{T}}$ and $[\xi(0), e(0), \tau(0)]^{\mathrm{T}} = [0, 0, 0]^{\mathrm{T}}$. It can be seen that the states x_1 and x_2 converge to zero gradually (Fig. 3b). This implies that the hybrid system is asymptotically stable and reflects the effectiveness of the proposed control strategy.

Again, to compare the effectiveness of our proposed dynamic output-feedback controller with that of a static output-feedback controller, consider a static output-feedback controller designed as $u = K\bar{y}$. To compare these two control strategies more fairly, we take $K = D_{\mathrm{c}} = -21.6673$ and the same event-triggered condition in the static output-feedback method as those in the dynamic case. The simulations results in Figs. 3c and 3d show that the evolutions of states in the dynamic output-feedback control system have shorter convergence time. One intuitive reason for this phenomenon is that different from the static output-feedback controller, the dynamic output-feedback controller introduces an auxiliary variable ξ which contains the memory information of y and hence guarantees a more effective control result.

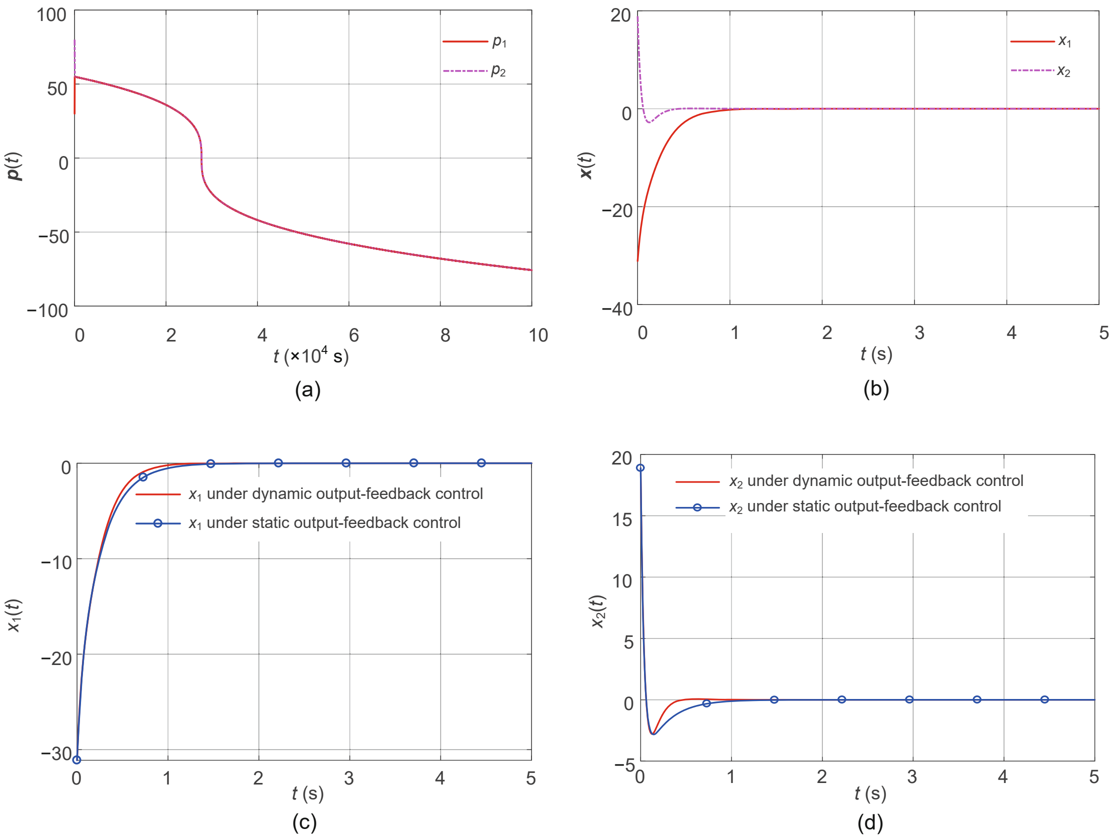

Fig. 3 Simulation results of Example 2: (a) evolutions of $p(t)$ of the genetic regulatory network system; (b) evolutions of $x(t)$ of the closed-loop error system under event-triggered dynamic output-feedback control; (c) evolutions of $x_1(t)$ under dynamic output-feedback (red line) and static output-feedback (blue-circle line) control; (d) evolutions of $x_2(t)$ under dynamic output-feedback (red line) and static output-feedback (blue-circle line) control. References to color refer to the online version of this figure

5 Conclusions

In this paper, we addressed the problem of dynamic output-feedback control for a class of Lipschitz nonlinear systems. Both continuous-time dynamic output-feedback control and event-triggered dynamic output-feedback control have been investigated for such Lipschitz nonlinear systems. For the continuous-time dynamic output-feedback control strategy, sufficient conditions for stability of the obtained closed-loop system have been established. In addition, for the event-triggered dynamic output-feedback control strategy, based on the design of the dynamic output-feedback controller gains and the event-triggered conditions, a hybrid system has been presented. Sufficient conditions have been proposed to ensure the stability of the hybrid system and an upper bound of the minimum inter-event interval has been provided to avoid the Zeno phenomenon. Finally, simulation results of two control strategy classes for nonlinear systems have been provided to confirm the efficiency of the proposed results.

One of our future research topics will be the study of robust event-triggered dynamic output-feedback control for nonlinear systems with external disturbance. In addition, the extension of the theoretical results to generalized Lipschitz systems is another future topic.

Contributors

Zhiqian LIU and Xuyang LOU designed the research. Zhiqian LIU processed the data. Zhiqian LIU and Xuyang LOU drafted the paper. Jiajia JIA helped organize and polish the paper. Zhiqian LIU and Xuyang LOU revised and finalized the paper.

Compliance with ethics guidelines

Zhiqian LIU, Xuyang LOU, and Jiajia JIA declare that they have no conflict of interest.

References

Abdelrahim M, Postoyan R, Daafouz J, et al., 2016. Stabilization of nonlinear systems using event-triggered output feedback controllers. *IEEE Trans Automat Contr*, 61(9):2682-2687. https://doi.org/10.1109/tac.2015.2502145

Andrieu V, Praly L, 2009. A unifying point of view on output feedback designs for global asymptotic stabilization. *Automatica*, 45(8):1789-1798. https://doi.org/10.1016/j.automatica.2009.04.015

Angulo MT, Moog CH, Liu YY, 2019. A theoretical framework for controlling complex microbial communities. *Nat Commun*, 10(1):1045. https://doi.org/10.1038/s41467-019-08890-y

Casey R, de Jong H, Gouzé JL, 2006. Piecewise-linear models of genetic regulatory networks: equilibria and their stability. *J Math Biol*, 52(1):27-56. https://doi.org/10.1007/s00285-005-0338-2

Chen J, Chen BM, Sun J, 2019. Complex system and intelligent control: theories and applications. *Front Inform Technol Electron Eng*, 20(1):1-3. https://doi.org/10.1631/FITEE.1910000

Chen PN, Cheng DZ, Jiang ZP, 2006. A constructive approach to local stabilization of nonlinear systems by dynamic output feedback. *IEEE Trans Automat Contr*, 51(7):1166-1171. https://doi.org/10.1109/tac.2006.878753

Collins EG, Selekwa MAF, Walker RB, et al., 2006. A stacked model structure for off-line parameter variation estimation in multi-equilibria nonlinear systems. *Eur J Contr*, 12(4):353-364. https://doi.org/10.3166/ejc.12.353-364

Dong JX, Yang GH, 2008. Dynamic output feedback control synthesis for continuous-time T-S fuzzy systems via a switched fuzzy control scheme. *IEEE Trans Syst Man Cybern B Cybern*, 38(4):1166-1175. https://doi.org/10.1109/tsmcb.2008.923530

Donkers MCF, Heemels WPMH, 2012. Output-based event-triggered control with guaranteed $\mathcal{L}_\infty$-gain and improved and decentralized event-triggering. *IEEE Trans Automat Contr*, 57(6):1362-1376. https://doi.org/10.1109/tac.2011.2174696

Ekramian M, 2020. Static output feedback problem for Lipschitz nonlinear systems. *J Franklin Inst*, 357(3):1457-1472. https://doi.org/10.1016/j.jfranklin.2019.10.031

Goebel R, Sanfelice RG, Teel AR, 2012. Hybrid Dynamical Systems: Modeling, Stability, and Robustness. Princeton University Press, Princeton, USA.

Gu Z, Huan Z, Yue D, et al., 2018. Event-triggered dynamic output feedback control for networked control systems with probabilistic nonlinearities. *Inform Sci*, 457-458:99-112. https://doi.org/10.1016/j.ins.2018.05.007

Hamid SR, Nazir MS, Rehan M, et al., 2019. New results on regional observer-based stabilization for locally Lipschitz nonlinear systems. *Chaos Solit Fract*, 123:173-184. https://doi.org/10.1016/j.chaos.2019.04.004

Kammogne AST, Kountchou MN, Kengne R, et al., 2020. Polynomial robust observer implementation based passive synchronization of nonlinear fractional-order systems with structural disturbances. *Front Inform Technol Electron Eng*, 21(9):1369-1386. https://doi.org/10.1631/FITEE.1900430

Khalil HK, 2014. Nonlinear Control, Global Edition. Pearson Education, USA.

Li FF, Sun JT, 2010. Asymptotic stability of a genetic network under impulsive control. *Phys Lett A*, 374(31-32):3177-3184. https://doi.org/10.1016/j.physleta.2010.05.054

Liu S, Song Y, Wei GL, et al., 2017. Event-triggered dynamic output feedback RMPC for polytopic systems with redundant channels: input-to-state stability. *J Franklin Inst*, 354(7):2871-2892. https://doi.org/10.1016/j.jfranklin.2017.02.008

Liu W, Wang ZM, Dai HH, et al., 2016. Dynamic output feedback control for fast sampling discrete-time singularly perturbed systems. *IET Contr Theory Appl*, 10(15):1782-1788. https://doi.org/10.1049/iet-cta.2016.0121

Meslem N, Prieur C, 2015. Event-based controller synthesis by bounding methods. *Eur J Contr*, 26:12-21. https://doi.org/10.1016/j.ejcon.2015.09.004

Molaei B, 2008. Optimization of dynamic output feedback controller for piecewise affine systems: an LMI approach. *J Circ Syst Comput*, 17(2):263-277. https://doi.org/10.1142/s021812660800423x

Nesic D, Teel AR, Carnevale D, 2009. Explicit computation of the sampling period in emulation of controllers for nonlinear sampled-data systems. *IEEE Trans Automat Contr*, 54(3):619-624. https://doi.org/10.1109/tac.2008.2009597

Park JH, 2005. On design of dynamic output feedback controller for GCS of large-scale systems with delays in interconnections: LMI optimization approach. *Appl Math Comput*, 161(2):423-432. https://doi.org/10.1016/j.amc.2003.12.037

Peng C, Yang TC, 2013. Event-triggered communication and $\mathcal{H}_\infty$ control co-design for networked control systems. *Automatica*, 49(5):1326-1332. https://doi.org/10.1016/j.automatica.2013.01.038

Pertew AM, Marquez HJ, Zhao Q, 2006. $\mathcal{H}_\infty$ observer design for Lipschitz nonlinear systems. *IEEE Trans Automat Contr*, 51(7):1211-1216. https://doi.org/10.1109/tac.2006.878784

Pham TP, Sename O, Dugard L, 2019. Unified $\mathcal{H}_\infty$ observer for a class of nonlinear Lipschitz systems: application to a real ER automotive suspension. *IEEE Contr Syst Lett*, 3(4):817-822. https://doi.org/10.1109/lcsys.2019.2919813

Qian CJ, Lin W, 2001. A continuous feedback approach to global strong stabilization of nonlinear systems. *IEEE Trans Automat Contr*, 46(7):1061-1079. https://doi.org/10.1109/9.935058

Qiu JL, 2007. Exponential stability of impulsive neural networks with time-varying delays and reaction–diffusion terms. *Neurocomputing*, 70(4-6):1102-1108. https://doi.org/10.1016/j.neucom.2006.08.003

Rehan M, Jameel A, Ahn CK, 2018. Distributed consensus control of one-sided Lipschitz nonlinear multiagent systems. *IEEE Trans Syst Man Cybern Syst*, 48(8):1297-1308. https://doi.org/10.1109/tsmc.2017.2667701

Sanchez EN, Perez JP, 2003. Input-to-state stabilization of dynamic neural networks. *IEEE Trans Syst Man Cybern A Syst Hum*, 33(4):532-535. https://doi.org/10.1109/tsmca.2003.811509

Shu F, Zhai JY, 2020. Event-triggered practical finite-time output feedback stabilisation for switched non-linear time-delay systems. *IET Contr Theory Appl*, 14(6):824-833. https://doi.org/10.1049/iet-cta.2019.1093

Tabuada P, 2007. Event-triggered real-time scheduling of stabilizing control tasks. *IEEE Trans Automat Contr*, 52(9):1680-1685. https://doi.org/10.1109/tac.2007.904277

Theodosis D, Dimarogonas DV, 2019. Event-triggered control of nonlinear systems with updating threshold. *IEEE Contr Syst Lett*, 3(3):655-660. https://doi.org/10.1109/lcsys.2019.2915719

Wang ZD, Qiao H, Burnham KJ, 2002. On stabilization of bilinear uncertain time-delay stochastic systems with Markovian jumping parameters. *IEEE Trans Automat Contr*, 47(4):640-646. https://doi.org/10.1109/9.995042

Yu H, Antsaklis PJ, 2013. Event-triggered output feedback control for networked control systems using passivity: achieving $\mathcal{L}_2$ stability in the presence of communication delays and signal quantization. *Automatica*, 49(1):30-38. https://doi.org/10.1016/j.automatica.2012.09.005

Zhang JH, Feng G, 2014. Event-driven observer-based output feedback control for linear systems. *Automatica*, 50(7):1852-1859. https://doi.org/10.1016/j.automatica.2014.04.026

Zhang XM, Han QL, 2016. A decentralized event-triggered dissipative control scheme for systems with multiple sensors to sample the system outputs. *IEEE Trans Cybern*, 46(12):2745-2757. https://doi.org/10.1109/TCYB.2015.2487420

Zhang XM, Han QL, 2017. Event-triggered $\mathcal{H}_\infty$ control for a class of nonlinear networked control systems using novel integral inequalities. *Int J Robust Nonl Contr*, 27(4):679-700. https://doi.org/10.1002/rnc.3598

Zhang Z, Li HP, Shi Y, et al., 2020. Cooperative optimal control for Lipschitz nonlinear systems over generally directed topologies. *Automatica*, 122:109279. https://doi.org/10.1016/j.automatica.2020.109279

Zhou J, Wen CY, Li TS, 2012. Adaptive output feedback control of uncertain nonlinear systems with hysteresis nonlinearity. *IEEE Trans Automat Contr*, 57(10):2627-2633. https://doi.org/10.1109/tac.2012.2190208

Zuo ZY, Lin ZL, Ding ZT, 2016. Truncated prediction output feedback control of a class of Lipschitz nonlinear systems with input delay. *IEEE Trans Circ Syst II Expr Briefs*, 63(8):788-792. https://doi.org/10.1109/tcsii.2016.2531053

Appendix: Proof of Theorem 1

Suppose that there exist positive definite matrices $\boldsymbol{X}_1$, $\boldsymbol{X}_2$, $\boldsymbol{Q}_1$, $\boldsymbol{Q}_2$, and matrices $\bar{\boldsymbol{A}}_{\mathrm{c}}$, $\bar{\boldsymbol{B}}_{\mathrm{c}}$, $\bar{\boldsymbol{C}}_{\mathrm{c}}$, $\bar{\boldsymbol{D}}_{\mathrm{c}}$ with appropriate dimensions such that LMI (5) is satisfied. Then, consider a Lyapunov function

$$V=V_1+V_2=\boldsymbol{x}^{\mathrm{T}}\bar{\boldsymbol{P}}_1\boldsymbol{x}+\boldsymbol{\xi}^{\mathrm{T}}\bar{\boldsymbol{P}}_2\boldsymbol{\xi},$$

where $\bar{\boldsymbol{P}}_1=\operatorname{diag}(\boldsymbol{X}_1,\boldsymbol{X}_2)$ and $\bar{\boldsymbol{P}}_2$ are symmetric positive definite matrices. To prove that system (4) is globally asymptotically stable, it suffices to show that the derivative $\dot{V}$ is negative definite. To this end, calculating the derivatives of V_1 and V_2 along with Eq. (4) yields

$$\begin{aligned}\dot{V}_1=&\dot{\boldsymbol{x}}^{\mathrm{T}}\bar{\boldsymbol{P}}_1\boldsymbol{x}+\boldsymbol{x}^{\mathrm{T}}\bar{\boldsymbol{P}}_1\dot{\boldsymbol{x}}\\=&[(\boldsymbol{A}+\boldsymbol{E}\boldsymbol{D}_{\mathrm{c}}\boldsymbol{C})\boldsymbol{x}+\boldsymbol{B}f(\boldsymbol{x})+\boldsymbol{E}\boldsymbol{C}_{\mathrm{c}}\boldsymbol{\xi}]^{\mathrm{T}}\bar{\boldsymbol{P}}_1\boldsymbol{x}\\&+\boldsymbol{x}^{\mathrm{T}}\bar{\boldsymbol{P}}_1[(\boldsymbol{A}+\boldsymbol{E}\boldsymbol{D}_{\mathrm{c}}\boldsymbol{C})\boldsymbol{x}+\boldsymbol{B}f(\boldsymbol{x})+\boldsymbol{E}\boldsymbol{C}_{\mathrm{c}}\boldsymbol{\xi}]\\=&\boldsymbol{x}^{\mathrm{T}}[(\boldsymbol{A}+\boldsymbol{E}\boldsymbol{D}_{\mathrm{c}}\boldsymbol{C})^{\mathrm{T}}\bar{\boldsymbol{P}}_1+\bar{\boldsymbol{P}}_1(\boldsymbol{A}+\boldsymbol{E}\boldsymbol{D}_{\mathrm{c}}\boldsymbol{C})]\boldsymbol{x}\\&+2f^{\mathrm{T}}(\boldsymbol{x})\boldsymbol{B}^{\mathrm{T}}\bar{\boldsymbol{P}}_1\boldsymbol{x}+2\boldsymbol{\xi}^{\mathrm{T}}\boldsymbol{C}_{\mathrm{c}}^{\mathrm{T}}\boldsymbol{E}^{\mathrm{T}}\bar{\boldsymbol{P}}_1\boldsymbol{x},\\\dot{V}_2=&\dot{\boldsymbol{\xi}}^{\mathrm{T}}\bar{\boldsymbol{P}}_2\boldsymbol{\xi}+\boldsymbol{\xi}^{\mathrm{T}}\bar{\boldsymbol{P}}_2\dot{\boldsymbol{\xi}}\\=&(\boldsymbol{A}_{\mathrm{c}}\boldsymbol{\xi}+\boldsymbol{B}_{\mathrm{c}}\boldsymbol{C}\boldsymbol{x})^{\mathrm{T}}\bar{\boldsymbol{P}}_2\boldsymbol{\xi}+\boldsymbol{\xi}^{\mathrm{T}}\bar{\boldsymbol{P}}_2(\boldsymbol{A}_{\mathrm{c}}\boldsymbol{\xi}+\boldsymbol{B}_{\mathrm{c}}\boldsymbol{C}\boldsymbol{x})\\=&\boldsymbol{\xi}^{\mathrm{T}}(\boldsymbol{A}_{\mathrm{c}}^{\mathrm{T}}\bar{\boldsymbol{P}}_2+\bar{\boldsymbol{P}}_2\boldsymbol{A}_{\mathrm{c}})\boldsymbol{\xi}+2\boldsymbol{x}^{\mathrm{T}}\boldsymbol{C}^{\mathrm{T}}\boldsymbol{B}_{\mathrm{c}}^{\mathrm{T}}\bar{\boldsymbol{P}}_2\boldsymbol{\xi}.\end{aligned}\tag{A1}$$

By means of inequality (2) and Lemma 1, we have

$$\begin{aligned}&2f^{\mathrm{T}}(\boldsymbol{x})\boldsymbol{B}^{\mathrm{T}}\bar{\boldsymbol{P}}_1\boldsymbol{x}\\\leq&\boldsymbol{x}^{\mathrm{T}}\bar{\boldsymbol{P}}_1\boldsymbol{B}\boldsymbol{Q}^{-1}\boldsymbol{B}^{\mathrm{T}}\bar{\boldsymbol{P}}_1\boldsymbol{x}+f^{\mathrm{T}}(\boldsymbol{x})\boldsymbol{Q}f(\boldsymbol{x})\\\leq&\boldsymbol{x}^{\mathrm{T}}\bar{\boldsymbol{P}}_1\boldsymbol{B}\boldsymbol{Q}^{-1}\boldsymbol{B}^{\mathrm{T}}\bar{\boldsymbol{P}}_1\boldsymbol{x}+\boldsymbol{x}^{\mathrm{T}}\boldsymbol{L}\boldsymbol{Q}\boldsymbol{L}\boldsymbol{x}\\=&\boldsymbol{x}^{\mathrm{T}}(\bar{\boldsymbol{P}}_1\boldsymbol{B}\boldsymbol{Q}^{-1}\boldsymbol{B}^{\mathrm{T}}\bar{\boldsymbol{P}}_1+\boldsymbol{L}\boldsymbol{Q}\boldsymbol{L})\boldsymbol{x},\end{aligned}\tag{A2}$$

where $\boldsymbol{Q}=\operatorname{diag}(\boldsymbol{Q}_1,\boldsymbol{Q}_2)$ is a positive definite matrix. Substituting inequality (A2) into Eq. (A1), we have

$$\begin{aligned}\dot{V}=&\dot{V}_1+\dot{V}_2\\\leq&\boldsymbol{x}^{\mathrm{T}}[(\boldsymbol{A}+\boldsymbol{E}\boldsymbol{D}_{\mathrm{c}}\boldsymbol{C})^{\mathrm{T}}\bar{\boldsymbol{P}}_1+\bar{\boldsymbol{P}}_1(\boldsymbol{A}+\boldsymbol{E}\boldsymbol{D}_{\mathrm{c}}\boldsymbol{C})\\&+\bar{\boldsymbol{P}}_1\boldsymbol{B}\boldsymbol{Q}^{-1}\boldsymbol{B}^{\mathrm{T}}\bar{\boldsymbol{P}}_1+\boldsymbol{L}\boldsymbol{Q}\boldsymbol{L}]\boldsymbol{x}\\&+2\boldsymbol{x}^{\mathrm{T}}\boldsymbol{C}^{\mathrm{T}}\boldsymbol{B}_{\mathrm{c}}^{\mathrm{T}}\bar{\boldsymbol{P}}_2\boldsymbol{\xi}+\boldsymbol{\xi}^{\mathrm{T}}(\boldsymbol{A}_{\mathrm{c}}^{\mathrm{T}}\bar{\boldsymbol{P}}_2+\bar{\boldsymbol{P}}_2\boldsymbol{A}_{\mathrm{c}})\boldsymbol{\xi}\\&+2\boldsymbol{\xi}^{\mathrm{T}}\boldsymbol{C}_{\mathrm{c}}^{\mathrm{T}}\boldsymbol{E}^{\mathrm{T}}\bar{\boldsymbol{P}}_1\boldsymbol{x}\\=&\boldsymbol{\zeta}^{\mathrm{T}}\tilde{\boldsymbol{P}}\boldsymbol{\zeta},\end{aligned}\tag{A3}$$

where $\boldsymbol{\zeta}=\operatorname{col}(\boldsymbol{x},\boldsymbol{\xi})$,

$$\tilde{\boldsymbol{P}}=\begin{bmatrix}\boldsymbol{\Theta}_1 & \bar{\boldsymbol{P}}_1\boldsymbol{E}\boldsymbol{C}_{\mathrm{c}}+\boldsymbol{C}^{\mathrm{T}}\boldsymbol{B}_{\mathrm{c}}^{\mathrm{T}}\bar{\boldsymbol{P}}_2\\ * & \boldsymbol{A}_{\mathrm{c}}^{\mathrm{T}}\boldsymbol{P}_2+\bar{\boldsymbol{P}}_2\boldsymbol{A}_{\mathrm{c}}\end{bmatrix}.$$

Herein $\boldsymbol{\Theta}_1=(\boldsymbol{A}+\boldsymbol{E}\boldsymbol{D}_{\mathrm{c}}\boldsymbol{C})^{\mathrm{T}}\bar{\boldsymbol{P}}_1+\bar{\boldsymbol{P}}_1(\boldsymbol{A}+\boldsymbol{E}\boldsymbol{D}_{\mathrm{c}}\boldsymbol{C})+\boldsymbol{L}\boldsymbol{Q}\boldsymbol{L}+\boldsymbol{P}_1\boldsymbol{B}\boldsymbol{Q}^{-1}\boldsymbol{B}^{\mathrm{T}}\boldsymbol{P}_1$. Therefore, if $\tilde{\boldsymbol{P}}<0$, the closed-loop system (4) is globally asymptotically stable. $\tilde{\boldsymbol{P}}$ can be rewritten as

$$\tilde{\boldsymbol{P}} = \begin{bmatrix} \boldsymbol{\Theta}_{11} & \bar{\boldsymbol{P}}_1\boldsymbol{E}\boldsymbol{C}_\mathrm{c} + \boldsymbol{C}^\mathrm{T}\boldsymbol{B}_\mathrm{c}^\mathrm{T}\bar{\boldsymbol{P}}_2 \\ * & \boldsymbol{A}_\mathrm{c}^\mathrm{T}\bar{\boldsymbol{P}}_2 + \bar{\boldsymbol{P}}_2\boldsymbol{A}_\mathrm{c} \end{bmatrix} + \begin{bmatrix} \bar{\boldsymbol{P}}_1\boldsymbol{B} \\ \boldsymbol{0} \end{bmatrix} \boldsymbol{Q}^{-1} \begin{bmatrix} \boldsymbol{B}^\mathrm{T}\bar{\boldsymbol{P}}_1 & \boldsymbol{0} \end{bmatrix},$$

where $\boldsymbol{\Theta}_{11} = (\boldsymbol{A}+\boldsymbol{E}\boldsymbol{D}_\mathrm{c}\boldsymbol{C})^\mathrm{T}\bar{\boldsymbol{P}}_1 + \bar{\boldsymbol{P}}_1(\boldsymbol{A}+\boldsymbol{E}\boldsymbol{D}_\mathrm{c}\boldsymbol{C}) + \boldsymbol{LQL}$. Using Lemma 2, it follows that $\tilde{\boldsymbol{P}} < 0$ is equivalent to

$$\begin{bmatrix} \boldsymbol{\Theta}_{11} & \bar{\boldsymbol{P}}_1^\mathrm{T}\boldsymbol{E}\boldsymbol{C}_\mathrm{c} + \boldsymbol{C}^\mathrm{T}\boldsymbol{B}_\mathrm{c}^\mathrm{T}\bar{\boldsymbol{P}}_2 & \bar{\boldsymbol{P}}_1\boldsymbol{B} \\ * & \boldsymbol{A}_\mathrm{c}^\mathrm{T}\boldsymbol{P}_2 + \bar{\boldsymbol{P}}_2\boldsymbol{A}_\mathrm{c} & \boldsymbol{0} \\ * & * & -\boldsymbol{Q} \end{bmatrix} < 0. \quad \text{(A4)}$$

Obviously, expression (A4) is a bilinear matrix inequality (BMI) problem which may be difficult to solve. Next, we convert and decompose the matrices in BMI (A4). Note that

$$\begin{aligned} &(\boldsymbol{A}+\boldsymbol{E}\boldsymbol{D}_\mathrm{c}\boldsymbol{C})^\mathrm{T}\bar{\boldsymbol{P}}_1 \\ &= \begin{bmatrix} \boldsymbol{A}_1^\mathrm{T} & (\boldsymbol{A}_3+\boldsymbol{D}_\mathrm{c}\boldsymbol{C}_1)^\mathrm{T} \\ \boldsymbol{A}_2^\mathrm{T} & (\boldsymbol{A}_4+\boldsymbol{D}_\mathrm{c}\boldsymbol{C}_2)^\mathrm{T} \end{bmatrix} \begin{bmatrix} \boldsymbol{X}_1 & \boldsymbol{0} \\ \boldsymbol{0} & \boldsymbol{X}_2 \end{bmatrix} \\ &= \begin{bmatrix} \boldsymbol{A}_1^\mathrm{T}\boldsymbol{X}_1 & (\boldsymbol{A}_3+\boldsymbol{D}_\mathrm{c}\boldsymbol{C}_1)^\mathrm{T}\boldsymbol{X}_2 \\ \boldsymbol{A}_2^\mathrm{T}\boldsymbol{X}_1 & (\boldsymbol{A}_4+\boldsymbol{D}_\mathrm{c}\boldsymbol{C}_2)^\mathrm{T}\boldsymbol{X}_2 \end{bmatrix}, \\ &\bar{\boldsymbol{P}}_1^\mathrm{T}\boldsymbol{E}\boldsymbol{C}_\mathrm{c} + \boldsymbol{C}^\mathrm{T}\boldsymbol{B}_\mathrm{c}^\mathrm{T}\bar{\boldsymbol{P}}_2 \\ &= \begin{bmatrix} \boldsymbol{X}_1 & \boldsymbol{0} \\ \boldsymbol{0} & \boldsymbol{X}_2 \end{bmatrix} \begin{bmatrix} \boldsymbol{0} \\ \boldsymbol{I} \end{bmatrix} \boldsymbol{C}_\mathrm{c} + \begin{bmatrix} \boldsymbol{C}_1^\mathrm{T} \\ \boldsymbol{C}_2^\mathrm{T} \end{bmatrix} \boldsymbol{B}_\mathrm{c}^\mathrm{T}\bar{\boldsymbol{P}}_2 \\ &= \begin{bmatrix} \boldsymbol{C}_1^\mathrm{T}\boldsymbol{B}_\mathrm{c}^\mathrm{T}\bar{\boldsymbol{P}}_2 \\ \boldsymbol{X}_2\boldsymbol{C}_\mathrm{c} + \boldsymbol{C}_2^\mathrm{T}\boldsymbol{B}_\mathrm{c}^\mathrm{T}\bar{\boldsymbol{P}}_2 \end{bmatrix}, \end{aligned}$$

$$\begin{aligned} \boldsymbol{LQL} &= \begin{bmatrix} \boldsymbol{L}_1 & \boldsymbol{0} \\ \boldsymbol{0} & \boldsymbol{L}_2 \end{bmatrix} \begin{bmatrix} \boldsymbol{Q}_1 & \boldsymbol{0} \\ \boldsymbol{0} & \boldsymbol{Q}_2 \end{bmatrix} \begin{bmatrix} \boldsymbol{L}_1 & \boldsymbol{0} \\ \boldsymbol{0} & \boldsymbol{L}_2 \end{bmatrix} \\ &= \begin{bmatrix} \boldsymbol{L}_1\boldsymbol{Q}_1\boldsymbol{L}_1 & \boldsymbol{0} \\ \boldsymbol{0} & \boldsymbol{L}_2\boldsymbol{Q}_2\boldsymbol{L}_2 \end{bmatrix}, \\ \bar{\boldsymbol{P}}_1\boldsymbol{B} &= \begin{bmatrix} \boldsymbol{X}_1 & \boldsymbol{0} \\ \boldsymbol{0} & \boldsymbol{X}_2 \end{bmatrix} \begin{bmatrix} \boldsymbol{B}_1 & \boldsymbol{B}_2 \\ \boldsymbol{B}_3 & \boldsymbol{B}_4 \end{bmatrix} \\ &= \begin{bmatrix} \boldsymbol{X}_1\boldsymbol{B}_1 & \boldsymbol{X}_1\boldsymbol{B}_2 \\ \boldsymbol{X}_2\boldsymbol{B}_3 & \boldsymbol{X}_2\boldsymbol{B}_4 \end{bmatrix}. \end{aligned}$$

Therefore, BMI (A4) can be converted into

$$\begin{bmatrix} \boldsymbol{\omega}_{11} & \boldsymbol{\omega}_{12} & \boldsymbol{\omega}_{13} & \boldsymbol{X}_1\boldsymbol{B}_1 & \boldsymbol{X}_1\boldsymbol{B}_2 \\ * & \boldsymbol{\omega}_{22} & \boldsymbol{\omega}_{23} & \boldsymbol{X}_2\boldsymbol{B}_3 & \boldsymbol{X}_2\boldsymbol{B}_4 \\ * & * & \boldsymbol{\omega}_{33} & \boldsymbol{0} & \boldsymbol{0} \\ * & * & * & -\boldsymbol{Q}_1 & \boldsymbol{0} \\ * & * & * & * & -\boldsymbol{Q}_2 \end{bmatrix} < 0, \quad \text{(A5)}$$

where

$$\begin{aligned} \boldsymbol{\omega}_{11} &= \boldsymbol{A}_1^\mathrm{T}\boldsymbol{X}_1 + \boldsymbol{X}_1\boldsymbol{A}_1 + \boldsymbol{L}_1\boldsymbol{Q}_1\boldsymbol{L}_1, \\ \boldsymbol{\omega}_{12} &= (\boldsymbol{A}_3+\boldsymbol{D}_\mathrm{c}\boldsymbol{C}_1)^\mathrm{T}\boldsymbol{X}_2 + \boldsymbol{X}_1\boldsymbol{A}_2, \\ \boldsymbol{\omega}_{13} &= \boldsymbol{C}_1^\mathrm{T}\boldsymbol{B}_c^\mathrm{T}\bar{\boldsymbol{P}}_2, \\ \boldsymbol{\omega}_{22} &= (\boldsymbol{A}_4+\boldsymbol{D}_\mathrm{c}\boldsymbol{C}_2)^\mathrm{T}\boldsymbol{X}_2 + \boldsymbol{X}_2(\boldsymbol{A}_4+\boldsymbol{D}_\mathrm{c}\boldsymbol{C}_2) \\ &\quad + \boldsymbol{L}_2\boldsymbol{Q}_2\boldsymbol{L}_2, \\ \boldsymbol{\omega}_{23} &= \boldsymbol{X}_2\boldsymbol{C}_\mathrm{c} + \boldsymbol{C}_2^\mathrm{T}\boldsymbol{B}_\mathrm{c}^\mathrm{T}\bar{\boldsymbol{P}}_2, \\ \boldsymbol{\omega}_{33} &= \boldsymbol{A}_c^\mathrm{T}\bar{\boldsymbol{P}}_2 + \bar{\boldsymbol{P}}_2\boldsymbol{A}_\mathrm{c}. \end{aligned}$$

Let $\bar{\boldsymbol{A}}_\mathrm{c} = \bar{\boldsymbol{P}}_2\boldsymbol{A}_\mathrm{c}$, $\bar{\boldsymbol{B}}_\mathrm{c} = \bar{\boldsymbol{P}}_2\boldsymbol{B}_\mathrm{c}$, $\bar{\boldsymbol{C}}_\mathrm{c} = \boldsymbol{X}_2\boldsymbol{C}_\mathrm{c}$, $\bar{\boldsymbol{D}}_\mathrm{c} = \boldsymbol{X}_2\boldsymbol{D}_\mathrm{c}$. Then inequality (A5) is equivalent to LMI (5). Moreover, let $\bar{\boldsymbol{P}}_2 = q^{-1}\boldsymbol{I}$. Then we can adjust the parameters of the controller by q as Eq. (6). This ends the proof of Theorem 1.